

University of Louisville

ThinkIR: The University of Louisville's Institutional Repository

Electronic Theses and Dissertations

5-2015

Vitamin A is essential for proper embryonic submandibular salivary gland growth.

Deanna Ellene Buenger
University of Louisville

Follow this and additional works at: <https://ir.library.louisville.edu/etd>



Part of the [Oral Biology and Oral Pathology Commons](#)

Recommended Citation

Buenger, Deanna Ellene, "Vitamin A is essential for proper embryonic submandibular salivary gland growth." (2015). *Electronic Theses and Dissertations*. Paper 2158.
<https://doi.org/10.18297/etd/2158>

This Master's Thesis is brought to you for free and open access by ThinkIR: The University of Louisville's Institutional Repository. It has been accepted for inclusion in Electronic Theses and Dissertations by an authorized administrator of ThinkIR: The University of Louisville's Institutional Repository. This title appears here courtesy of the author, who has retained all other copyrights. For more information, please contact thinkir@louisville.edu.

VITAMIN A IS ESSENTIAL FOR PROPER EMBRYONIC SUBMANDIBULAR
SALIVARY GLAND GROWTH

By

Deanna Ellene Buenger

A Thesis

Submitted to the Faculty of the
School of Dentistry at the University of Louisville
In Partial Fulfillment of the Requirements

for the degree of

Master of Science
in Oral Biology

Department of Molecular, Cell and Craniofacial Biology
University of Louisville
Louisville, Kentucky

May 2015

VITAMIN A IS ESSENTIAL FOR PROPER EMBRYONIC SUBMANDIBULAR
SALIVARY GLAND GROWTH

By Deanna Ellene Buenger

A Thesis approved on
April 24, 2015

Lisa L. Sandell, Ph.D. – Mentor/Director

Douglas S. Darling, Ph.D. - Committee Member

Brian Shumway, DDS- Committee Member

Dennis Warner, Ph.D. - Committee Member

ACKNOWLEDGEMENTS

I would like to thank Dr. Lisa Sandell for allowing me to work and learn in her lab during my time at the University of Louisville. It has been an honor to work under such an accomplished and dedicated investigator and scientist. Your patience and guidance over the past two years is greatly appreciated. I know I have learned a great deal and hope that I can take several new assets forward with me in my future endeavors.

I would also like to thank Diana Hadel, for teaching and assisting me with new procedures as well as answering my numerous questions. Your patience and encouragement are greatly appreciated and without you this project would not be at completion.

I would also like to extend my appreciation to my committee members, Dr. Douglas Darling, Dr. Brian Shumway and Dr. Dennis Warner. The time and dedication given to me for my committee meetings as well as constructive feedback were valuable to my time here. In addition, my committee members were always willing to loan me lab equipment and antibodies. I really appreciate the generosity of both time and resources given to me to allow me to complete my research.

ABSTRACT

VITAMIN A IS ESSENTIAL FOR PROPER EMBRYONIC SUBMANDIBULAR SALIVARY GLAND GROWTH

Deanna E. Buenger

April 24, 2015

Submandibular salivary glands (SMG) are important for the production of saliva. Salivary glands may be damaged by autoimmune disease, surgery, or radiation therapy. Retinoic acid (RA) is a signaling metabolite derived from Vitamin A that is essential for proper embryonic growth and development; specifically for cardiovascular, limb and craniofacial development. The goal of this study was to determine if there is a reproducible defect in the growth of SMGs in RA deficient mouse embryos compared to wild type. This study aims to characterize SMG growth in RA deficient embryos and determine if the growth could be stimulated by RA in a dose dependent manner. In addition, we hypothesized that there was a direct effect of the RA deficiency on SMG growth using an *in vitro* model. We examined *Rdh10* mutant mouse embryos: which lack the enzyme retinol dehydrogenase necessary to produce RA. We examined the SMGs of

wild type and *Rdh10* mutant embryos by hematoxylin and eosin staining at various stages of gland development. We then completed whole mount antibody staining for the epithelium (E-cadherin) and nerve (TUJ), and compared the volumes of these glands. We also varied the dosage of all-*trans*-retinal (RAL), the intermediate in RA metabolism, supplementation to determine how this affects SMG growth. The mutant SMGs were approximately half the size of the wild type SMGs at both the early stage of gland development and further into development. With the higher dose of RAL, the mutant SMGs appeared more like the wild type, with branching and near normal SMG size. In order to see if RA directly affected SMG growth, wild type SMGs were cultured *in vitro* for up to 72 hours. SMGs treated with a synthetic Retinoic acid receptor (RAR) inhibitor (BMS 493) had less epithelium and branching compared to the control SMGs. Together, the results of these analyses demonstrate that RA directly affects SMG growth: specifically the epithelial growth and differentiation are influenced by the presence and dosage of RA.

TABLE OF CONTENTS

Acknowledgements.....	iii.
Abstract	iv.
List of Tables.....	viii.
List of Figures.....	ix.
Chapter 1: Introduction and Background.....	1
1.1 Salivary Gland Overview.....	1
1.2 Causes of Salivary Gland Damage.....	2
1.3 Potential Therapies for Salivary Hypofunction.	3
1.4 Submandibular Salivary Gland Development.....	4
1.5 Vitamin A Metabolism in the Developing Embryo.....	8
1.6 Study Hypothesis.....	13
Chapter 2: Materials and Methods.....	14
2.1 Maternal Supplementation.....	14
2.2 Euthanasia and Dissection.....	14
2.3 Paraffin Embedding and Sectioning.....	15
2.4 Hematoxylin and Eosin Staining	16

2.5 Whole Gland Dissection of SMGs.....	17
2.6 Antibody Staining for Whole Mount SMG.....	17
2.7 Antibody Staining for Paraffin Sections.....	18
2.8 Antibodies.....	20
2.9 Culturing SMGs <i>in vitro</i>	21
2.10 Statistical Analysis.....	21
Chapter 3: Results.....	23
Chapter 4: Discussion and Conclusion.....	68
References.....	71
Curriculum Vitae.....	73

LIST OF TABLES

i. T-test analysis of E12.5 Cross Section Area	30
ii. E15.5 Cross Section Area Analysis Data.....	35
iii. Cultured Glands <i>in vitro</i> Data.....	60
iv. T-test Table for Cultured SMGs (48 hrs.).....	61

LIST OF FIGURES

1. Developmental Stages of the SMG.....	7
2. Vitamin A Metabolism.....	9
3. Vitamin A Metabolism for <i>RDH10</i> ^{tr^{ex}/tr^{ex}} Mutants.....	12
4. H and E Staining of E12.5 SMGs.....	25
5. H and E staining/Statistical data for E12.5.....	26
6. Proportions of H and E E12.5.....	28
7. H and E Staining of E15.5 SMGs.....	32
8. H and E staining/Statistical data for E15.5.....	33
9. Antibody Staining of E15.5 Cross Section.....	37
10. E13.5 Whole Mount 2D Images from Confocal (4 mg RAL).....	38
11. E13.5 Volume Calculation Example.....	40
12. E 13.5 Whole Mount 3D Images from Confocal (4 mg RAL).....	41
13. Whole Mount Statistics – Volume as a proportion.....	42
14. Vitamin A Metabolism Allows for Adjustment and Higher Dosage of RAL.....	44
15. Representation of RAL Dosage Increase Effect.....	45
16. E13.5 Whole Mount 2D images (15 mg RAL).....	46
17. E13.5 Whole Mount 3D images (15 mg RAL).....	48
18. Whole Mount Statistics –as a proportion (15 mg RAL).....	49
19. PSP Antibody Staining- Cell Differentiation.....	50
20. PSP images.....	52

21. Cultured SMGs- 48 hours.....	53
22. Counting End Buds of Cultured SMGs.....	55
23. Cultured Glands Statistical Analysis –numbers.....	56
24. Cultured Glands Statistical Analysis-Proportion.....	57
25. Cultured Glands -72 hours.....	58
26. Antibody Staining of Cultured Glands (Ecad only).....	62
27. Antibody Staining of Cultured Glands (Ecad and PH3).....	64
28. Quantifying Cell Proliferation in Cultured Glands.....	65
29. Statistical Analysis on Cultured glands for Cell Proliferation.....	67

CHAPTER 1: INTRODUCTION AND LITERATURE REVIEW

Salivary Gland Overview

Saliva has many essential roles within the oral cavity. Aside from the main purpose of providing lubrication for digestion and swallowing, saliva is also essential as a pH buffer for the oral tissue, as well as aiding in vocalization [1, 2]. Saliva is produced by three main pairs of salivary glands, in addition to thousands of minor salivary glands [3]. The main pairs of salivary glands include the submandibular gland, the sublingual gland, both of which are located in the mandible at the base of the tongue, and the parotid gland, located anterior to the ears overlying the masseter muscle. Healthy adults produce around 1.5 liters of saliva per day, which, aside from comfort and convenience, is necessary to protect the teeth from decay causing microorganisms [4]. However, perhaps the true value and importance of saliva is only appreciated by patients who suffer from defective salivary glands and hyposalivation.

Damaged salivary glands result in a severe dry mouth condition called xerostomia. Xerostomia can be caused by surgical damage to the glands, autoimmune disease, (e.g. Sjögren's syndrome) or radiation therapy. Hyposalivation can induce dental caries and periodontal disease [3]. In addition, decreased saliva production results in problems with speech, mastication, and overall quality of life. Currently, there is no

effective treatment for xerostomia, therefore most patients only receive medication for pain management and substitute saliva or lubricants to help cope with this devastating condition [5]. Additional treatments include preventing dental caries with antimicrobials, as well as sialagogues agents to aid in saliva output [6].

Causes of Salivary Gland Damage

One of the most common causes of salivary gland damage is Sjögren's syndrome. Sjögren's syndrome is one of the most common autoimmune diseases, characterized by ocular and oral dryness as a result of the immune system degrading the lacrimal and salivary glands [7]. This autoimmune disease is estimated to affect 0.01% to 3% of the general population [8]. Primary Sjögren's syndrome occurs when it is the only autoimmune disease afflicting the patient[9], whereas secondary Sjögren's syndrome occurs in the presence of additional autoimmune disease. Patel notes that there is much controversy as to classification criteria of Sjögren's syndrome; resulting in the prevalence of this condition being most likely underestimated [9]. Doctors from around the world follow their own classification criteria for both primary and secondary Sjögren's syndrome. What can be agreed upon are the primary symptoms, including hyposalivation and oral dryness [8, 9]. Regardless of the classification and diagnosis of this condition, the result is decreased functional salivary gland tissue, leading to xerostomia.

Another major cause of xerostomia is radiation therapy, the often used treatment for head and neck cancer. According to the American Cancer Society, approximately 40,000 people will be diagnosed with head and neck cancer in 2015 in the United States

(www.cancer.org). If the cancer has spread to local lymph nodes, radiation therapy is the primary treatment. Because of the sensitivity of their tissue, salivary glands are often damaged by radiation [10]. The cells in salivary glands, including the SMG, have slow proliferation rates and highly differentiated cell composition. These cells are highly sensitive to radiation, however the effects are long term and may not peak until years after treatment [10]. Currently, the main method to protect the salivary glands from radiation therapy is through preventative measures. Such organ sparing procedures where salivary glands are relocated to a region which receives lower radiation dose [11]. Other preventative procedures include gene therapy to make the salivary glands more resistant to the radiation [11].

Potential Therapies for Salivary Gland Hypofunction

The goal of salivary gland research is to provide relief for patients suffering from defective salivary glands. Scientists are working towards bioengineering salivary glands from stem or progenitor cells [3, 11] in order to work towards regeneration of defective salivary glands [12]. Ogawa *et al.* was able to successfully regenerate salivary glands by use of a bioengineered germ layer of a mouse salivary gland [13]. This study shows an exciting proof of concept that a treatment for xerostomia could be bioengineering salivary glands to form replacement glands. However, to make this process more efficient and to be confident that the salivary gland is fully functioning, first we must understand how the salivary gland grows during embryonic development, providing a template for bioengineering a functional salivary gland [9]. In addition, it should be noted that many

questions remain about the functionality of transplanted stem cells. In order to achieve a successful transplant, it is necessary to determine the regenerative nature of specific cells, and how we can direct differentiation to lead to the highly specialized cells of the salivary gland [14].

Submandibular Salivary Gland Development

Embryonic development of the SMG is a complicated process with many signaling pathways, cell to cell interactions, and cell processes occurring at designated times. For proper gland development, growth and differentiation must both occur. These orchestrated events are necessary to form a functional and healthy gland [1, 15].

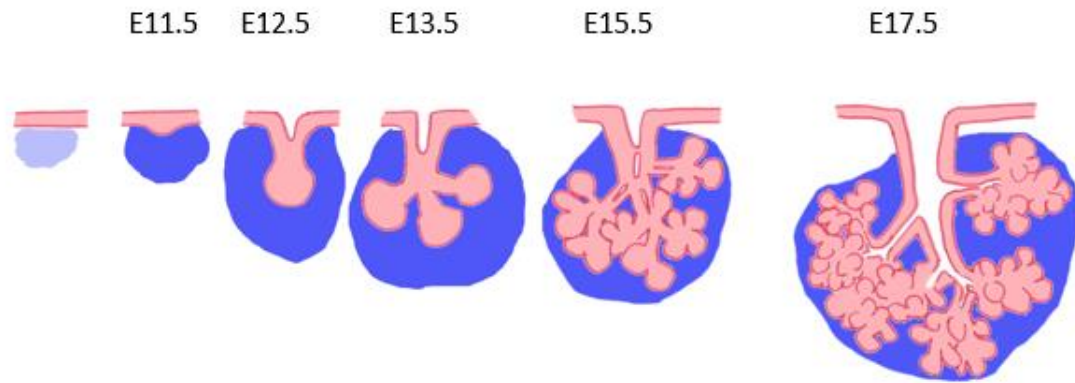
Researchers in the salivary gland field often study the SMG, as it is the first gland to develop during embryogenesis.

The submandibular gland is composed of both epithelial and mesenchymal tissue. During the earliest stages of development, the epithelium is the instructive tissue, guiding the mesenchyme towards the beginning of gland development [16], however this role is transferred to the mesenchyme in later developmental stages. The SMG produces both serous and mucous secretions, a unique feature compared to the other main salivary glands. The serous secretions contain digestive enzymes, such as amylase, which are necessary for breaking down food [6]. The mucous secretions provide the lubrication and viscosity of saliva, aiding in vocalization and swallowing, while also protecting the oral cavity from pathogens and oral flora that stimulate tooth decay. The developed SMG is composed of a series of ducts and branches of epithelial bundles. Branching

morphogenesis, a necessary feature in SMG development, is simply defined by the salivary epithelium undergoing repetitive sequences of branching to create buds and clefts [17]. These bundles are called acini and are formed from acinar cells. The acini are what secrete saliva into the ducts, which then empty into the oral cavity. At the earliest stage, around E11.5 (embryonic day 11.5), a signal, not yet identified, alerts the oral tissues where to form a SMG and a placode of epithelium begins to develop. By day E12.5 an initial bud stage occurs when the epithelium invaginates into the surrounding mesenchymal tissue to form the precursor for a salivary gland (fig 1.). The pseudoglandular stage occurs on E13.5, in which a few of the branches of epithelium begin to develop. By the canalicular stage, at E15.5, there are many more branches and the ducts and lumens begin forming through apoptosis and tubulogenesis [18]. The gland continues growing and branching even after it reaches the terminal bud stage on E17.5. The SMG does not reach full size until after birth and near puberty. Branching morphogenesis is essential to SMG development as it allows compact overall size yet has vast epithelial surface area which is crucial for the generation of large surface area to produce sufficient amounts of saliva [19].

Because salivary glands are complex organs, there are many cell processes, signaling pathways and tissue interactions that must be understood in order to fully comprehend their development. Also important to salivary gland development is parasympathetic innervation, which was recently discovered necessary for salivary glands to grow and branch correctly [20, 21]. Other research has found that FGF10 (fibroblast growth factor 10) signaling within the primordial epithelium is necessary for communication to the mesenchyme [20]. This tissue to tissue interaction is essential for

initiation and gland formation [16]. The mesenchyme is the instructive tissue from E11.5 and on through gland development. When mesenchyme is taken from the second pharyngeal arch and placed next to any developing epithelium,[16] it branches and looks similar to a developing salivary gland [16]. Other research has verified that Sonic Hedgehog (SHH) signaling is another essential developmental pathway necessary for salivary gland development [22]. FGF8 also plays a dose dependent role in epithelium development, although it does not work through the FGF10 signaling pathway [23]. These are just a handful of examples of the research going on in the salivary gland field. All of these projects contribute toward understanding the complexity of the salivary glands and how these signaling pathways interconnect and work in harmony in order to form a functional salivary gland.



E= Embryonic
Day of
Development

Image by Dr. Lisa Sandell, PhD

Figure 1: Developmental stages of the submandibular gland. Depicted in pink is epithelium, and the blue depicts the surrounding mesenchyme. Salivary gland development is first visible as a thickening of oral epithelium on E11.5. Next is the initial bud stage at E12.5, then the pseudoglandular stage on E13.5 shows some branching morphogenesis taking place. The canalicular stage around E15.5 is when the canals and lumens begin to form. Duct formation continues even throughout the terminal bud stage of E17.5.

Vitamin A Metabolism in the Developing Embryo

Vitamin A, the parent molecule of the Retinoids is inactive in this form [24]. In this inactive state, Vitamin A (Retinol) is stored in the liver and bone marrow of adults [23]. Before the body can use Vitamin A, it must be converted to its active form- Retinoic Acid (RA). During development, RA is a necessary signaling molecule needed to activate many developmental genes [25]. The metabolism of Retinol is a complex process involving first the oxidation of Retinol to all-*trans*-Retinal (fig 2.). Next, RAL is converted to the active form, RA, and can then activate many developmental genes. This step is carried out by the ALDH1a family of enzymes, when these specific family members are knocked out, we see RA deficiency in certain regions of the developing embryo [26]. RA acts as a ligand and binds to a family of receptors, RAR (Retinoic Acid Receptors) and RXR (Retinoid-x Receptors), which include multiple isoforms. These RA receptors are a part of the nuclear super family of receptors, which activate or inhibit downstream genes. The RAR heterodimerizes with RXR, and together this complex interacts with the promoter sequence of specific genes [27]. RA receptors are active and specific depending on the tissue and developmental stage involved [28]. The metabolism of Vitamin A is depicted below (fig.2).

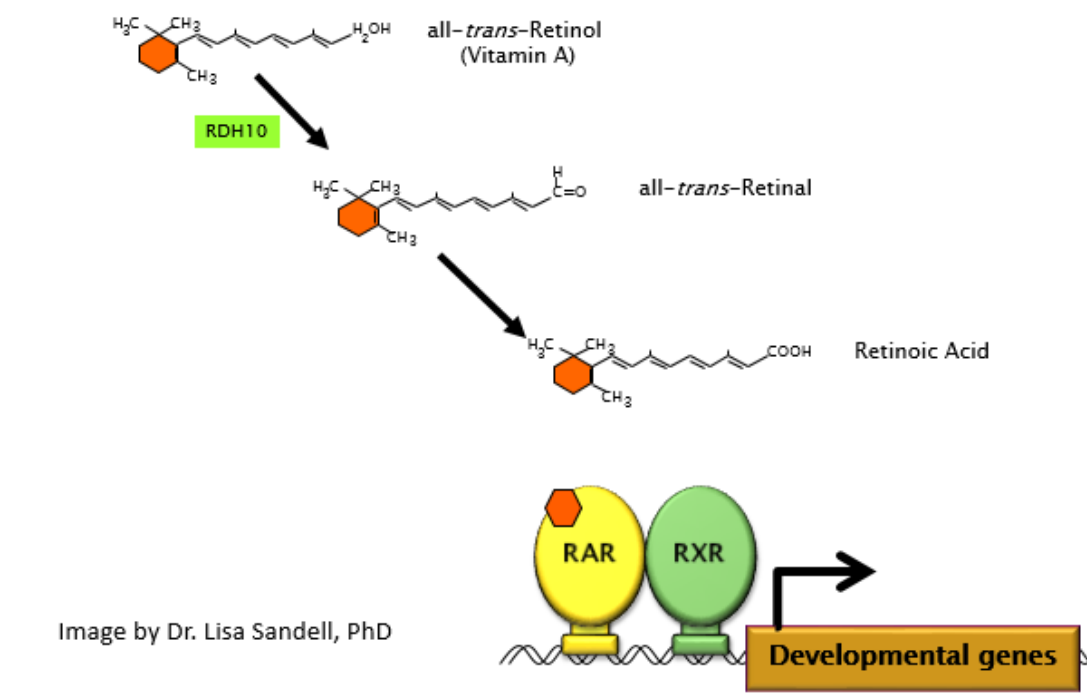


Figure 2. Vitamin A metabolism. The metabolism of Vitamin A converts Retinol into the active form called Retinoic Acid (RA). The first step in this process involves the RDH10 enzyme which oxidizes Retinol into the intermediate, RAL. From this step, RAL is then converted into RA, the active metabolite that activates many developmental genes. The ligand RA, activates the developmental genes by activating RAR (Retinoic Acid Receptors) and RXR (Retinoid X Receptors), as shown above.

RA has been shown to be essential during embryonic development [29]. RA dosage, interactions with other signaling pathways, involvement with cell processes such as proliferation and apoptosis and the developmental stage of RA's presence are all essential for organogenesis [25]. Common symptoms of Vitamin A deficiency during embryogenesis include lack of eye development, cleft palate, and arrested ascension of kidneys as well as cardiovascular defects [24, 27, 28, 30]. Vitamin A deficiency (VAD) symptoms are devastating, and often the embryo doesn't survive development and live to post-natal stages. Depending on the severity of VAD as well as the stage during gestation when the embryo is deprived, the embryos will often suffer cardiovascular fatality and resorb[26].

It was recently determined that one enzyme is primarily responsible for the first step in Vitamin A metabolism[26]. RDH10 (retinol dehydrogenase 10) oxidizes Retinol into RAL [25, 26]. This is a reversible step. Sandell *et al.* have developed a method to study RA deficient mouse embryos that survive to later stages of gestation, allowing the organs of interest to grow under VAD conditions [25, 26]. By using the intermediate formed during Vitamin A metabolism, RAL, maternal supplementation is used to keep the embryos alive [25]. The strain of animals used is *Rdh10^{rex/+}* heterozygotes. Based on Mendelian genetics, when one *Rdh10^{rex/+}* is crossed with another *Rdh10^{rex/+}* heterozygote, roughly 25% of the filial embryos are homozygous for the mutation. These mutants completely lack the enzyme RDH10, and therefore cannot metabolize Vitamin A. Normally with this level of RA deficiency, the mutant embryos would not survive past E11.5. However, with the maternal diet receiving the intermediate, RAL, enough RA is made to overcome cardiovascular fatality, allowing the embryos to survive (fig.3). If this

intermediate is given at the critical time for heart and lung development, embryos are rescued, allowing them to develop to the time of salivary gland development (fig. 3). This system salvages the embryos, and is a great benefit to allow us to study embryos under VAD conditions.

The Metabolism of Vitamin A

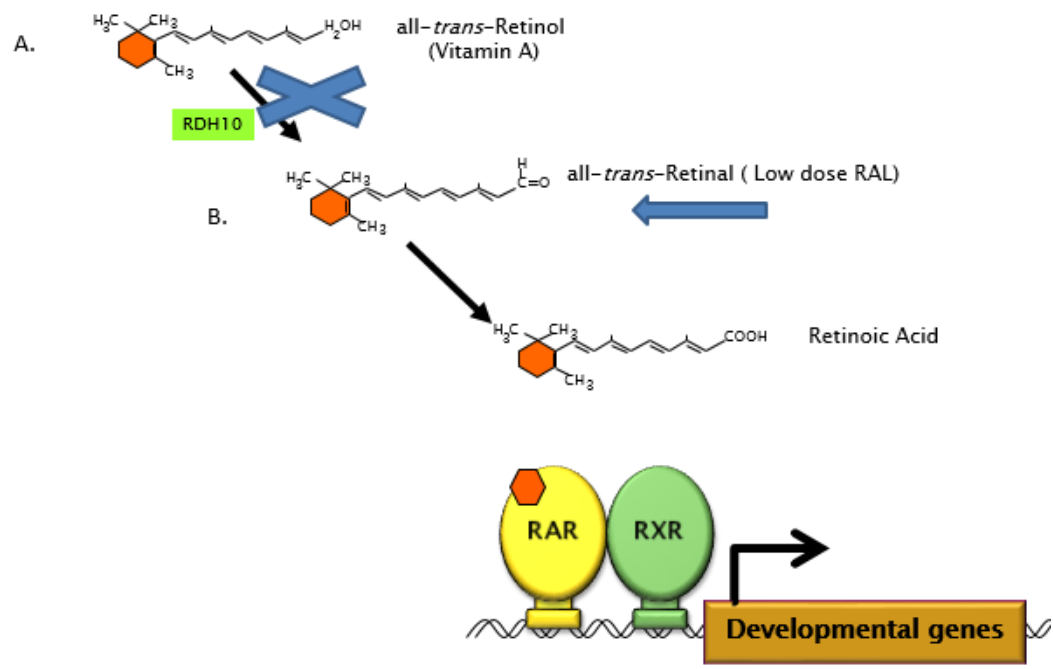


Figure 3. Vitamin A metabolism in the *Rdh10^{trax/trax}* mutant embryos. This image demonstrates that *Rdh10^{trax/trax}* mutant embryos lack the enzyme required for the first step in this metabolic pathway. With this level of RA deficiency, the mutant embryos will not survive. However, the innovation to this research rescues the *Rdh10^{trax/trax}* mutant embryos by giving a maternal supplementation of RAL. This allows the embryos to make enough RA to survive cardiovascular fatality. This process rescues the embryos, and allows them to survive to the time of SMG development, even with RA deficient conditions.

Study Hypothesis

There is much about salivary gland development and morphogenesis that is unknown. Understanding how the various signaling pathways interact, and at what times these communications need to take place during development is still being studied and learned. Preliminary data from Sandell *et al.* suggested that there was a growth defect in the RA deficient embryo's SMGs. The impact and role of RA on the developing SMG has not yet been studied. Because of the innovative maternal supplementation system, we can study the developing SMGs and allow the embryos to survive to the point of gland development. In this study we would like to see how RA levels affect SMG growth and differentiation to better understand how healthy, normal salivary glands mature. This project can contribute to science as we work toward regeneration and bioengineering of new salivary glands, as a treatment of defective salivary glands. It was hypothesized that RA is necessary for proper development of the embryonic SMG. The first aim was to show that there is indeed a reproducible growth defect in the RA deficient embryos. The next aim was to see if the epithelium is the tissue affected by the RA deficiency. The third aim was to evaluate if this growth defect is present at multiple stages of gland development, or only present at a specific time. This research gives us insight as to the role of RA on the developing SMG.

CHAPTER 2: MATERIALS AND METHODS

Maternal Supplementation:

All-trans-Retinal (RAL) (Sigma Chemical, St. Louis, MO) was prepared in a dark room and on a bed of ice. The RAL was suspended by diluting 4 mg of RAL per 80 microliters of filter sterilized Ethanol. This amount was aliquoted into light inhibiting (amber) Eppendorf tubes and stored at negative 20 degrees Celsius until the day it was used. Plugged dams received RAL treatments on embryonic day 7.5, 8.5, 9.5, 10.5, 11.5 and then the diet was changed to a clean cage with A5010 mouse food on the 12th day. Approximately 50g of 5010 mouse food was crushed using a mortar and pestle until it was finely ground. The food was added to a sterile plastic zip bag. A pipet was used to suspend the RAL into 50 ml of water. The water was inverted several times to ensure that the RAL was thoroughly mixed. The 50 ml of water and RAL was added to the bag with the crushed mouse food and mixed. The moist food was then deposited onto a sterile culture dish which was covered with a light blocking igloo (VWR, CA) to prevent light from degrading the RAL. This was placed in the mouse cage and was replaced every 24 hours.

The Euthanasia and Dissection:

The following animal protocols were approved by IACUC at the University of Louisville (#11116). Mice were euthanized using a CO₂ gas chamber. Cervical

dislocation was also performed to verify that the animal was deceased before beginning the embryo harvest. Embryos were dissected out of the mother and immediately put into a dish where they were submerged in 10 mM PBS (phosphate buffered saline). If embryonic day was equal to or greater than E15.5, the embryos were decapitated immediately. Upon completion of removing the embryonic sac, placenta and procuring a tissue sample for genotyping, embryos were fixed overnight in 4% Paraformaldehyde (PFA) at 4°C. Approximately 24 hours later, the embryos were dehydrated through a series of methanol washes. From PFA, the embryos were equilibrated to methanol following a series of 30 minutes washes.

Paraffin Embedding and Sectioning:

Tissues were dehydrated and prepared through 30 minute washes from the following procedure. Beginning from absolute ethanol, to 50:50 EtOH and Neo-Clear, to absolute Neo-Clear (2X). The tissues were then incubated for two hours in warm paraffin in the warming vacuum oven at the melting temperature for the paraffin used (58°C). After two hours, this paraffin was replaced with freshly melted paraffin and the tissues were incubated for another two hours in the vacuum oven. Each specimen was embedded in the frontal orientation by placing them in a mold filled with warm paraffin. The embedded specimen was then stored at 20°C for a minimum of a few hours, so that the paraffin could set. A microtome was used for the paraffin sectioning. The sectioning was carried out, placing the paraffin block on the machine and sections of 10 µm were created. The sections were floated in the warm water bath, then placed onto a clean

microscope slide. Slides were allowed to air dry overnight, then were put away and stored at room temperature until further analysis.

Hematoxylin and Eosin (H and E) Staining:

The protocol for Hematoxylin and Eosin staining of paraffin slides begins by dehydrating the tissues with two X 10 minute washes in xylene. Next, the slides were moved to two X 5 minute washes in 100% ethanol. After this step, the slides were moved stepwise through 95% ethanol, and 70% ethanol for 2 minute rinses. The paraffin slides were then submerged in hematoxylin for 8 minutes. The slides were then moved into a cold tap water bath for a 5 minute rinse. After this, the slides were placed for 30 seconds in 0.1% acid alcohol (J.T. Baker HCL) then were moved back into a cold tap water bath for an additional minute. After this, the slides were moved into a lithium carbonate solution for 45 seconds. This solution was prepared with approximately 1.3 g of lithium carbonate per 100 mL of distilled water. The slides were then rinsed in a running water bath for 5 minutes. Next, the paraffin slides had 10 quick dips in 80% ethanol before having 10 quick dips in eosin (Harleco, KS). After the eosin, the slides had a five minute wash in 95% ethanol then they were moved to absolute ethanol for two 5 minute washes. For the last step, the slides were placed in xylene for 5 minutes, and this was repeated two times. After the staining was complete, the slides were covered with coverslips, using permount and allowed to air dry.

Whole Gland Dissection of Submandibular Glands:

Timed mating's were set up using *Rdh10^{trax/+}* heterozygotes. When a vaginal plug was found, that day was counted as embryonic day 0.5. On the desired embryonic stage day, the dam was euthanized following the above procedure. The collected embryos were placed in 10 mM PBS for the dissection. The SMGs were dissected out from the mandible and were fixed in 4% PFA overnight. The next day, the tissues were rinsed in PBS and moved stepwise to absolute methanol.

Antibody Staining of Whole Mount SMG:

This is a three day procedure. Day 1: SMG specimens that had been stored in 100% methanol (MEOH) were incubated in Dent's Bleach for 2 hours at room temperature. Dent's Bleach is composed of MEOH: DMSO: 30%H₂O₂, 4:1:1. The glands were equilibrated to PBS, moving stepwise through the following solutions for 10 minutes each. The glands were then blocked in TN plus block for 2 hours (Perkin—Elmer with TSA kit). Next, the antibodies were prepared (see antibody section) diluted in TN+block and incubated overnight at 4°C.

Day 2: Unbound primary antibody was removed by washing five times for 1 hour in PBS. Secondary antibodies were diluted in TN+block and diluted antibodies were applied and specimens were incubated overnight at 4°C.

Day 3: Unbound secondary antibody was removed by washing in PBS for 20 minutes (3X). Bound antibody complexes were then fixed to the tissue by incubation for 1 hour in 4% PFA. Lastly, specimens were moved to PBS, and then equilibrated to MEOH.

Mounting antibody stained specimens for confocal imaging: A concave slide was used with vacuum grease to hold a plastic ring on the perimeter of indentation. BABB, a tissue clearing agent, was used to clear the tissue and then a slide cover was placed over the ring with BABB filled up to the rim.

Immunohistochemistry and Heat Induced Epitope Recovery for Paraffin sections:

Slides with paraffin sections were prewarmed in an oven (58°C) for 30 minutes in a glass rack. The slides were transferred quickly to xylene for 3 five minute washes and then were moved to 100% ethanol for 2 five minute wash. The slides were then placed in 95% ethanol for 3 two minute wash. Then move to 70% ethanol for a two minute wash, then two minutes in PBS.

HIER (Heat Induced Epitope Retrieval): Slides were placed in a 2 L beaker filled with about 400 mL of citrate buffer. Once visibly boiling for 10 minutes, the beaker was removed from heat and allowed to cool. At room temperature, the slides were immersed in PBS. A PAP pen was used to mark a hydrophobic perimeter around the tissue. Then the slide was washed twice with PBS, within the PAP pen circumference. PBS was then removed and the slide was blocked for 1 hour with 100-200 microliters of 10% calf serum (made in 0.1% triton) and stored in a humid box for the incubation.

Next, two quick washes with PBS were completed, followed by a rinse in PBS with 0.1% Triton. The primary antibodies were prepared by diluting them in the 4% calf serum in 0.1% Triton –PBS. Approximately 100-200 microliters of primary antibody was added to each slide over the sections. Slides with primary antibodies were incubated for

an hour in the humid box. To remove unbound primary antibodies, slides were washed 2X quickly in PBS/0.1% Triton, then were placed for five minutes in a wash of PBS/Triton (2X).

The secondary antibodies were prepared by diluting in 4% calf serum and then centrifuging for two minutes. Once prepared, about 100-200 microliters of the diluted secondary antibody was added to the slide over the sections. The slides were then incubated in the humid box for one hour. Next the slides were washed in PBS triton (five minutes) then two quick washes with PBS- Triton. The slides were covered using antifade gel (Invitrogen, NY) and stored in a light sensitive box. Reagents needed for this procedure included 10 mM citrate buffer, 0.1% Triton-PBS, 10% calf serum in .1% Triton PBS blocking solution and 4% calf serum in 0.1% Triton-PBS.

Antibodies:

Primary Antibodies:

- E-cadherin Mouse: BD Biosciences 610182. Dilution used [1:50].
- TUJ 1: Covance, 500017-641. Dilution used [1:1000].
- E-cadherin Rabbit: 3195-9. Dilution used [1:200].
- Phosphohistone 3(PH3): EMD Millipore Corp: 06-570. Dilution used [1:500].
- PSP: [31, 32]. Dilution used [1:100].

Secondary Antibodies:

- AF488: Donkey anti mouse IgG. Invitrogen A21202. Dilution used [1:300]
- AF488: Donkey anti rabbit IgG. Invitrogen A21206. Dilution used [1:300].
- AF546: Goat anti mouse IgG. Invitrogen A11030. Dilution used [1:300].
- AF546: Goat anti rabbit IgG. Invitrogen A11010. Dilution used [1:300].
- AF660: Goat anti rabbit. Invitrogen 421073. Dilution used [1:300].
- AF660: Goat anti mouse. Invitrogen A21055. Dilution used [1:300].

Culturing SMGs *in vitro*:

Wild type (FVB/NJ) mice were mated and embryos harvested at the desired embryonic day. Media was stored at -20°C, but freshly thawed DMEM (VWR, CA) in 37°C incubator for duration of harvest. SMGs were collected (preferably E13.5) and left in a dish of DMEM with Hepes, a pH buffer (VWR, CA).

Five ml of DMEM was pipetted (VWR, CA) into a culture dish. A filter was placed in the medium on a silicone raft, then a gland was placed on the top of the filter paper (VWR, CA). For control dishes, 14 µL DMSO was added to the media. For experimental dishes, the RAR antagonist BMS-493 (Tocris, United Kingdom) 14 µL was added to the media (10 nM-[33, 34]). The dishes were covered and placed in the incubator (5%CO₂ and 37°C) for 24, 48 or 72 hours. After the desired time in culture, the glands were fixed in 4% PFA overnight. Then the glands were moved stepwise to absolute methanol.

Statistical Analysis:

Statistical analysis can be used to determine if there is a significant difference between two groups of numbers. Student T-tests were completed (using Microsoft Excel software) to compare cross sectional area analysis data for the wild type and mutant numbers. In our case, this was used on the cross section area analysis for E12.5 and E15.5 SMG development from H and E stained sections. Graphs and histograms were also created on this program.

Nonparametric statistical analysis was completed on mini tab (www.minitab.com), a statistical software purchased through the University of Louisville. This nonparametric analysis was needed for small subsets of numbers, such as the volume comparison for the whole mount glands. The nonparametric test gives us the same information as the T-test however it does not assume normal distribution because the n value is small.

CHAPTER 3: RESULTS

Verify a reproducible growth defect in the SMG of RA deficient embryos.

In order to verify that there was a reproducible growth defect of the SMGs in the RA deficient embryos, pregnant mice were treated with a low dose of RAL to ensure their survival so that the RA deficient developing embryos would survive to the stage of salivary gland development. Embryos were collected (n=8, from two different litters) at E12.5, during the initial bud stage. This is the earliest stage that a defined gland could be detected, as the epithelium invaginates into the surrounding mesenchyme (fig.1). Embryos were fixed, dehydrated then prepared and embedded in paraffin. Embryos were embedded in the frontal orientation (fig.4). After paraffin sectioning, H and E staining was completed to allow the histology to be seen clearly. Very consistently, we saw smaller E12.5 glands in the homozygous *Rdh10^{trax/trax}* mutants compared to the wild type embryos (fig.4).

To verify that there was a true difference in size between the E12.5 mutant and wild type SMGs, a statistical analysis was completed on the paraffin sections. Taking the largest cross section of the gland, the area was calculated by using the Leica software (fig.5). As seen in the figure, only the epithelium cross-section area was calculated. Below is a graphical representation of the cross-sections areas. The size discrepancy is shown and was seen consistently throughout all of the glands.

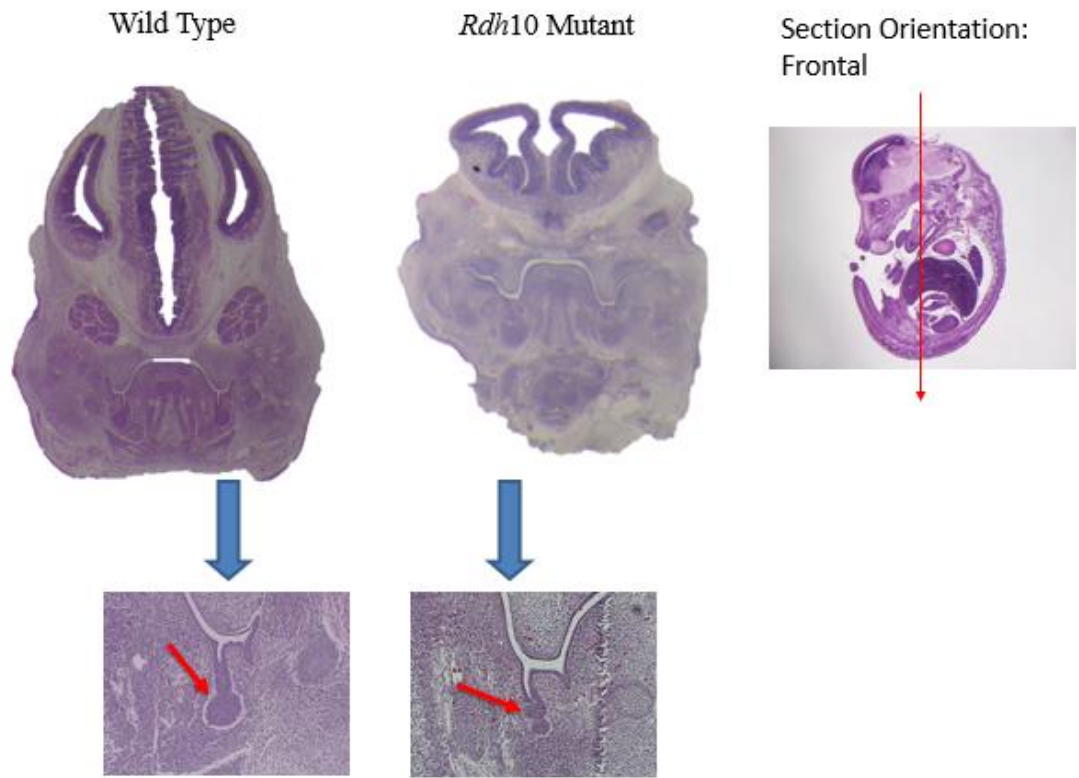


Figure 4. Hematoxylin and Eosin staining of E12.5 embryos. Above represents the frontal orientation paraffin sections and H and E staining of wild type and *Rdh10*^{tr^{ex}/tr^{ex}} embryos. At E12.5, initial bud stage, we see the *Rdh10* mutant (on right) SMG is visibly smaller than the wild type on the left, shown with the red arrows. For this H and E analysis, n=8 wild type glands and n=8 mutant glands. The above images are representative examples from the data.

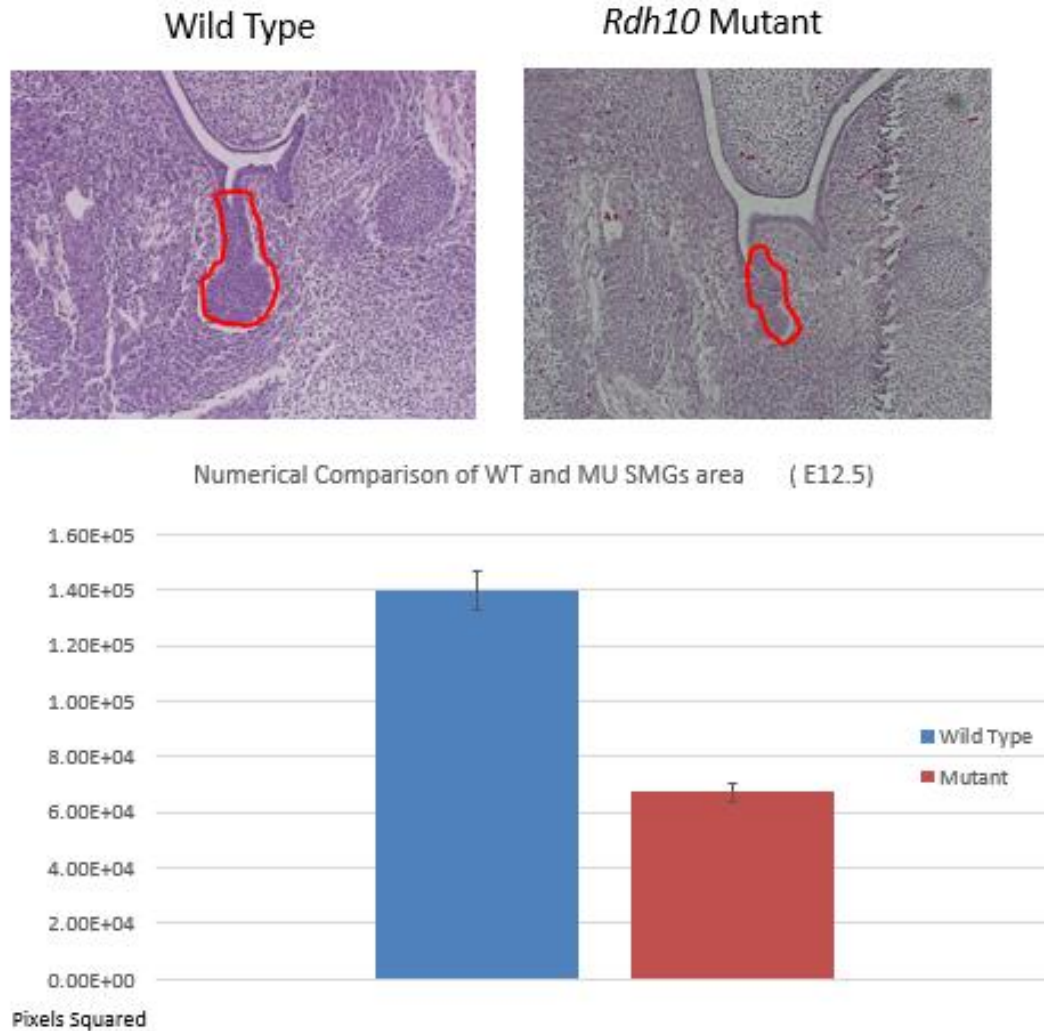


Figure 5. Hematoxylin and Eosin staining of E12.5 SMGs and statistical analysis. The above figure demonstrates the process of the statistical analysis of the cross sections of E12.5 SMGs. Taking the largest cross-section of the gland, Leica software was used to compute the area of the gland. The graph demonstrates the cross section areas as a histogram based on the whole numbers, units are in pixels squared (PX²). For the statistical analysis, n=8 for the wild type glands and n=8 for the mutant glands. The error bars show the standard deviation as calculated by Microsoft Excel. The calculated p value was 0.025 which is less than the α value of 0.05. The t test results indicate statistically significant cross section area difference between the mutant and wild type SMGs.

Another graphical representation was completed to look at the variation of the cross section of the glands as a proportion. The wild type cross section was normalized and that cross section area became 1. Therefore, fig. 6 (below) allows us to see that the initial bud SMG of *Rdh10* mutant embryos are approximately 50% the average cross section area compared to the wild type SMGs.

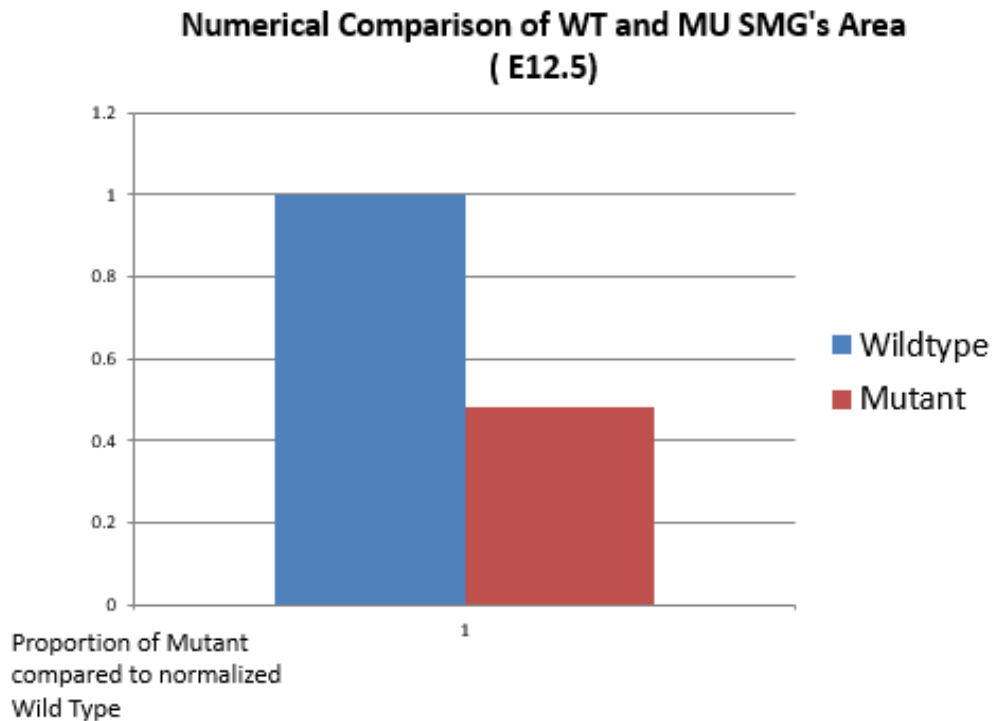


Figure 6. Graphical representation of E12.5 SMG cross section area analysis. This graph shows the cross section area of E12.5 SMGs normalized to the wild type average. The Y axis shows the proportion of the cross section area, with the wild type cross section area representing 1. Based on our data, the average mutant cross section area is near 50% the size compared to the wild type average cross sectional area. For this graphical representation, n=8 wild type glands and n=8 mutant glands. A student T-test was completed on this data, and verified that the difference between the mutant and wild type cross section area is statistically significant ($P < \alpha: 0.025 < 0.05$).

These data indicate that the RA deficient embryos SMG have a growth defect that is reproducible. Further statistical analysis was completed to show if there was a significant difference between the wild type and mutant cross section areas of the E12.5 SMGs. For the student t-test, n= 8 wild type SMGs and n=8 mutant SMGs. By looking at the results of the student T-Test, we see that the p-value (0.025) is less than the α value (0.05). This means we reject the null hypothesis, which states that there is no true difference between these groups of data (table 1.). Our data indicates that difference between the wild type cross section areas and the mutant cross section areas is significant and that this growth defect is indeed reproducible.

Area Analysis of E12.5 SMGs (Units is in Pixels Squared)

Wild Type	Mutant
204274.18	14258.96
49763.98	10642.61
128968	149480.6
134665.9	12871.56
119008	174782.6
124006	17086.41
165339.9	93298.89
192456.7	65451.89

T-Test: Two-Sample Assuming Equal Variances

	Variable 1	Variable 2
Mean	1	0.480896
Variance	0.12069	0.222854
Observations	8	8
Pooled Variance	0.171772	
Hypothesized Mean Difference	0	
Df	14	
t Stat	2.505003	
P(T<=t) one-tail	0.012611	
t Critical one-tail	2.624494	
P(T<=t) two-tail	0.025222	
t Critical two-tail	2.976843	

Table i. T-test analysis of E12.5 cross section area. Above is the T-Test results completed on the Microsoft Excel software. For this analysis, n=8 SMGs for both the wild type and mutant groups. We can interpret the data by comparing the p-value (0.025) to the α value (0.05). Because the p-value is less than the α value, we reject the null hypothesis that there is no difference between the two groups of data. Since we reject the null hypothesis, then we can accept the alternative hypothesis- which says that there is a difference between the wild type and mutant cross section areas. Therefore, the T-test shows that difference between the mutant average cross section areas compared to the wild type cross section area is significant.

Evaluate if the growth defect in the developing SMG of RA deficient embryos is present at a later stage

In order to see if this growth defect in the RA deficient embryos is present at later stages of SMG development, embryos were collected at E15.5 (the canalicular stage) and the similar process was followed as completed for the E12.5 embryos. As seen in fig. 7, the *Rdh10* mutant SMGs compared to the wild type SMGs still display a growth defect.

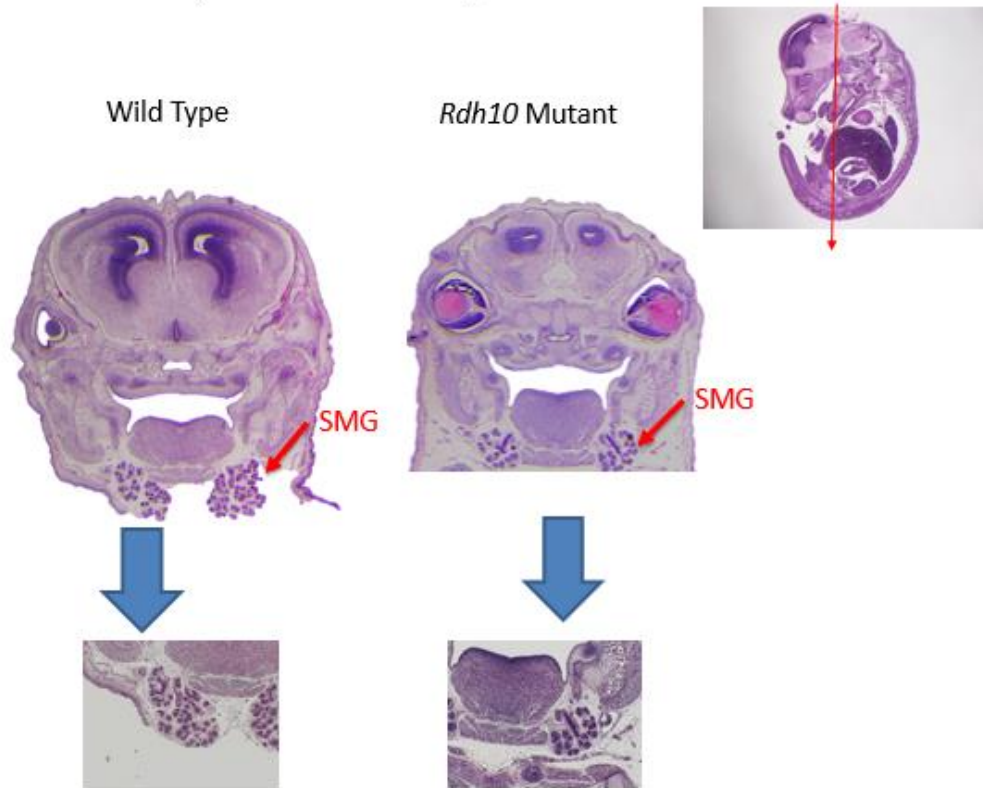


Figure 7. Hematoxylin and Eosin staining of E15.5 SMGs. In order to see if the growth defect in the RA deficient embryos continued to later stages of SMG development, embryos were collected at E15.5 (the canalicular stage) and the similar process was followed as completed for the E12.5 embryos. As seen in this figure, the *Rdh10* mutant SMG still displays a growth defect compared to the wild type littermate embryo, as shown with the red arrows.

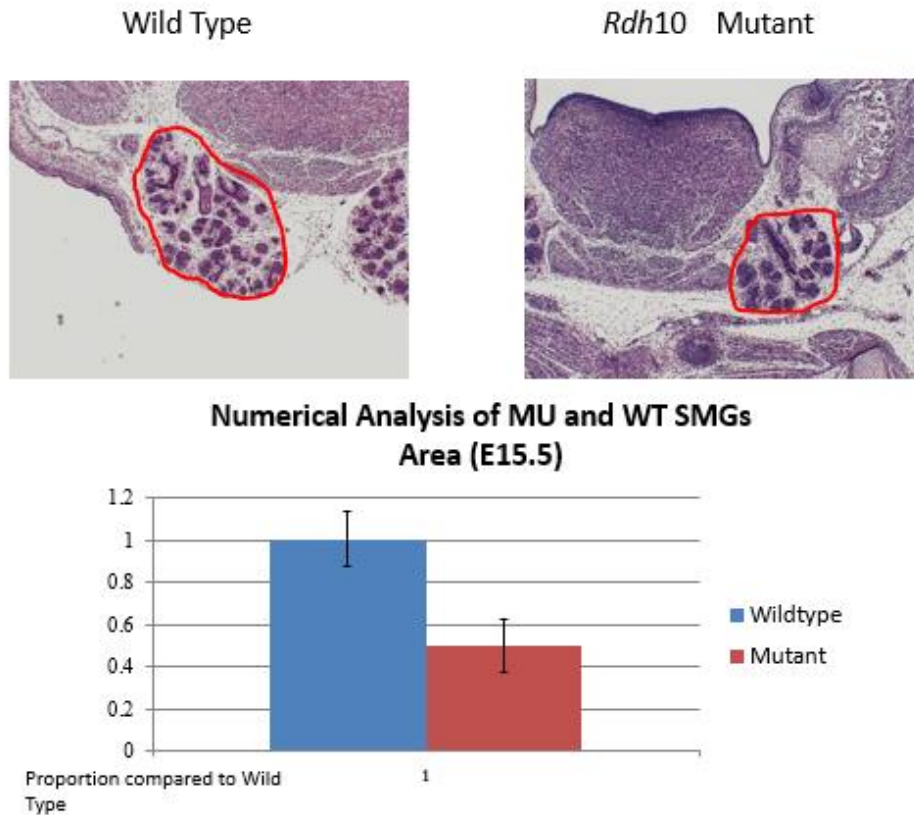


Figure 8. Hematoxylin and Eosin staining of E15.5 SMGs and statistical analysis. The figure above shows the statistical analysis for the canalicular stage E15.5, H and E stained paraffin slides. The largest cross section was studied. The Leica software calculated the cross section area of the SMG. The graph demonstrates the areas shown as a proportion, and the average wild type cross section area was normalized to represent 1. For this analysis, n=6 wild type glands and n=6 mutant glands. The error bars demonstrate the standard deviation. Based on student t-test results, our p value (0.00000274) is less than our α value (0.05), meaning that our data is statistically significant. We can see the growth defect of the RA deficient SMG is still present at E15.5, as the mutant cross section area is about 50% compared to the wild type.

In order to verify that there is a reproducible growth defect in E15.5 SMGs, further statistical analysis was completed. For each embryo (n=6, 2 litters), the largest cross section of the gland was stained and then, using Leica software, the cross sectional area was calculated (fig.8). Using the wild type SMGs as the normalized cross section area, we see the graphical representation of the mutant size compared to the wild type. Once again, we see a difference in growth of the SMGs in RA deficient embryos at the later developmental stage of E15.5. A T-test statistical analysis was completed to determine if the difference between the cross section areas of the mutant and wild type SMGs was significant. The finding is significant if the p-value (5.48E-06) is less than the α value (0.05). Our data (table 2) demonstrates that there is a statistical difference between the average cross section areas, comparing the wild type and mutant SMGs. Based on the H and E staining and analysis at E12.5 and E15.5, we see that the growth defect in RA deficient embryos is present at the early initial bud stage of gland development and also seen at the later canalicular stage.

Area Analysis of E15.5 SMGs (Units is in Pixels Squared)

Wild Type	Mutant
771720.285	515165.874
684234.9	225990.6
709840	399737.6
945058.13	373442.54
643872.572	329268.506
736636.913	385275.859

t-Test: Two-Sample Assuming Equal Variances

	<i>Variable</i> 1	<i>Variable</i> 2
Mean	748560.5	371480.2
Variance	9.31E+09	7.43E+09
Observations	6	6
Pooled Variance	8.37E+09	
Hypothesized Mean Difference	0	
Df	12	
t Stat	7.709608	
P(T<=t) one-tail	2.74E-06	
t Critical one-tail	2.680998	
P(T<=t) two-tail	5.48E-06	
t Critical two-tail	3.05454	

Table ii. Above is the T-test for the E15.5 SMG cross section area analysis data, as calculated by Microsoft Excel. The above table shows the calculated cross sectional areas of the E15.5 SMGs. The student t-test was completed, with n=6 for both wild type and mutant SMG data. Based on the T-test results, the p-value (5.48E-06) is less than the α value (0.05), indicating that there is a true difference between these groups of data. Therefore, we can conclude that the difference between the mutant and wild type cross section area, is significant.

In order to more clearly visualize the epithelium of the RA deficient SMGs, immunofluorescence antibody staining was used to highlight the epithelium of E15.5 paraffin sectioned embryos (frontal orientation). E-cadherin, shown in red, depicts the epithelium (fig.9). The *Rdh10* mutant glands are smaller in cross section area, as shown below, and this analysis shows that there is less epithelium in the mutant gland as well. This verifies that not only are the RA deficient SMGs smaller in cross sectional area but there is less epithelium in the glands.

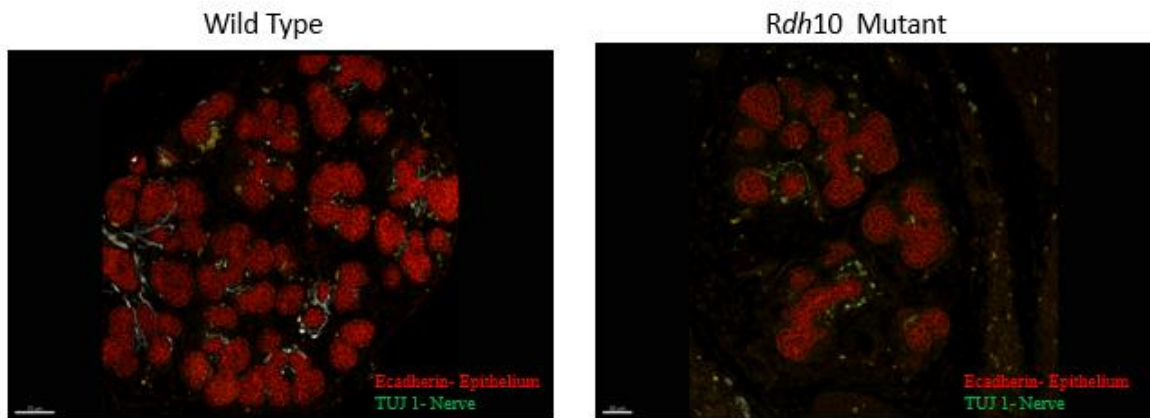


Figure 9. Immunofluorescence staining of E15.5 SMGs. This figure depicts the immunofluorescence staining of E15.5 paraffin section slides. Red demonstrates the epithelium, and the green highlights the nerve of the E15.5 SMGs. The mutant SMGs have less epithelium than wild type, and shown by the immunofluorescence staining.

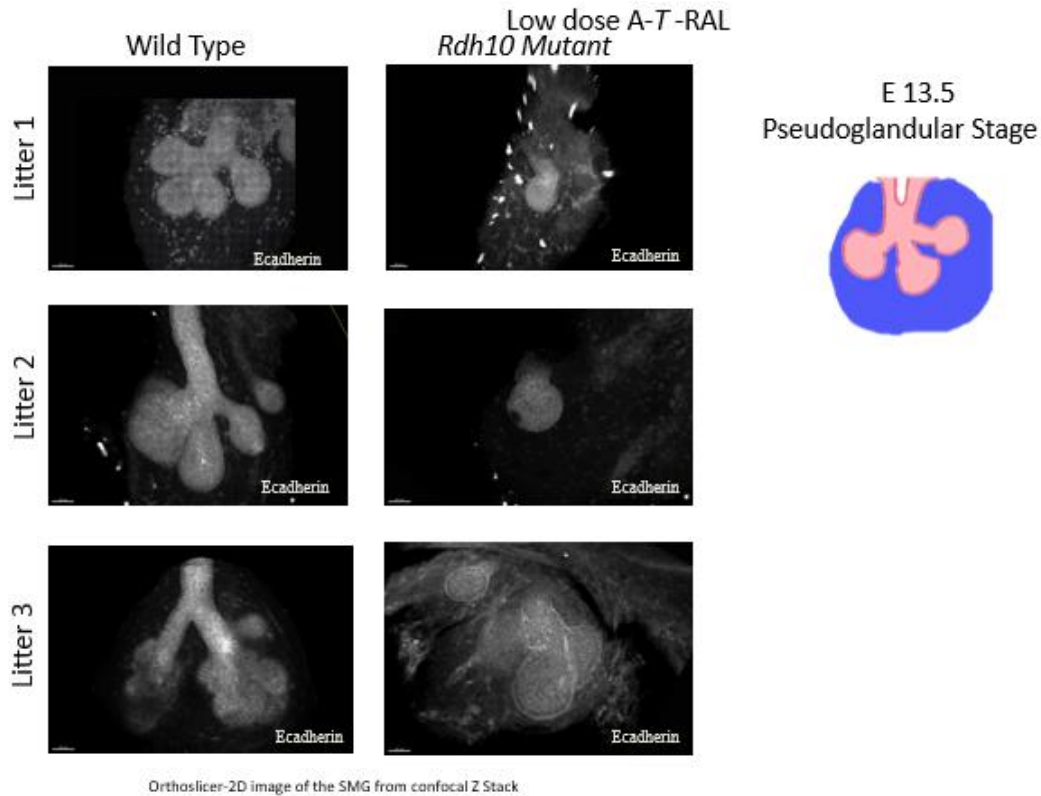


Figure 10. Whole mount images of E13.5 SMGs. The above figure shows the whole mount analysis of the E13.5 glands immunostained with E-cadherin to visualize epithelium. Figure 10 demonstrates the 2D representation of the gland taken on a confocal laser microscope. For this analysis, 3 separate litters were studied (n=3) with the wild type gland on the left and mutant gland shown on the right. On the far right is the cartoon depiction of the pseudoglandular stage SMG. This simple schematic shows the epithelium in pink and the mesenchyme in blue. At the pseudoglandular stage, we see a few epithelial buds and branching begin.

In order to accurately assess the growth defect of the RA deficient SMGs, we sought to measure the epithelial volume of *Rdh10^{trax/trax}* mutant SMG relative to wild type. In order to measure epithelial volume a whole mount gland analysis was completed using immunofluorescence and confocal laser microscopy imaging. SMGs were harvested at E13.5 and antibody staining for E-cadherin was completed. The confocal was used to capture both the 2D and 3D image of each gland. In order to look at variations among different litters, 3 different litters were analyzed for this data. Shown above (fig.10) is the 2D image taken from the confocal Z stack. The wild type gland for each litter is shown on the left and the mutant gland is shown on the right. For each litter, we see a growth defect in the epithelium. Using the Imaris software, volume was calculated for each gland by compiling the 2D epithelium boundaries from the z stack and forming a 3D surface (fig.11). Figure 12 depicts the 3D volume calculated from the rendered surface by the Imaris Software.

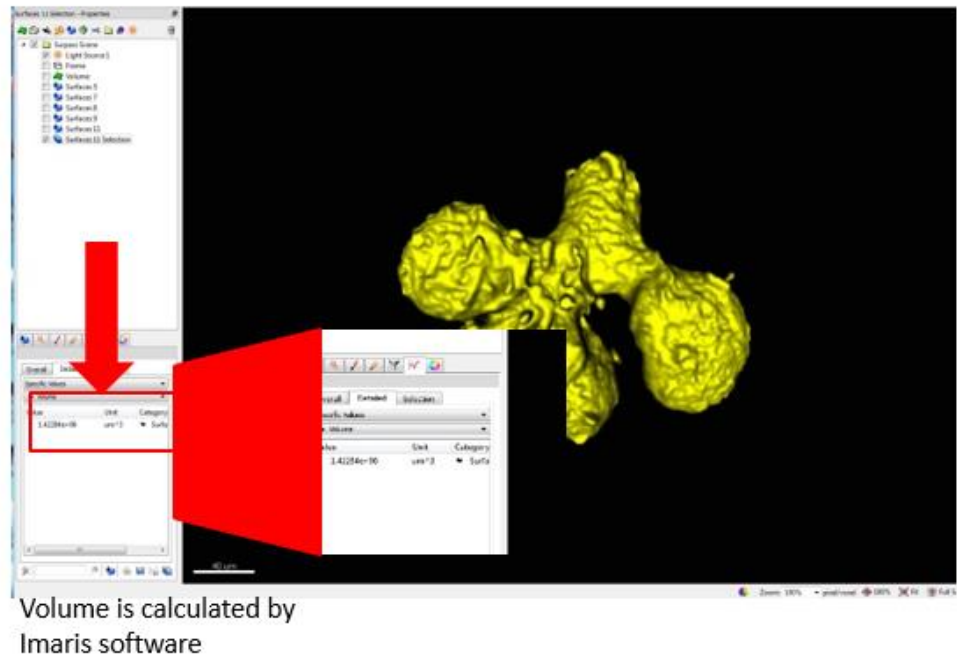
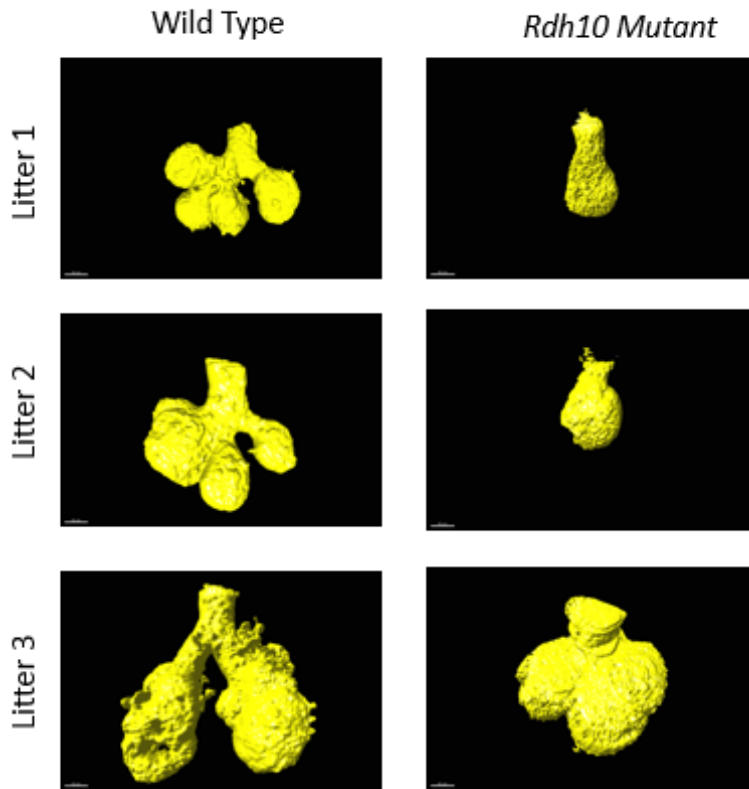


Figure 11. E13.5 SMGs whole mount analysis. The image above shows that the Imaris software compiled the confocal Z stack images to form a 3D representation of the E13.5 whole mount SMGs. The volume of the epithelium was calculated, and these volumes were used for further statistical analysis to compare the mutant and wild type SMG's volume.



Volume formed by compiling confocal Z Stacks, creating a 3D representation of the SMGs

4 mg RAL	litter 1	litter 2	litter 3
Wild Type Volume (μm^3)	1.42E+06	1.47E+06	5.88E+06
Mutant Volume (μm^3)	5.55E+05	5.89E+05	2.59E+06

Figure 12. E13.5 whole mount volume images (low dose RAL). The above figure shows the volume based on the compilation of the confocal Z-stacks, as formed by the Imaris software, and the units are in μm^3 . Shown below the volume images, are the actual calculated volumes of the E13.5 SMGs. These calculated volumes were used for statistical analysis, in which the Wilcoxon Signed Rank test verified a statistically significant difference between the mutant and wildtype SMGs volume. For this analysis, n=3 separate litters, and p (0.091) less than α (0.10).

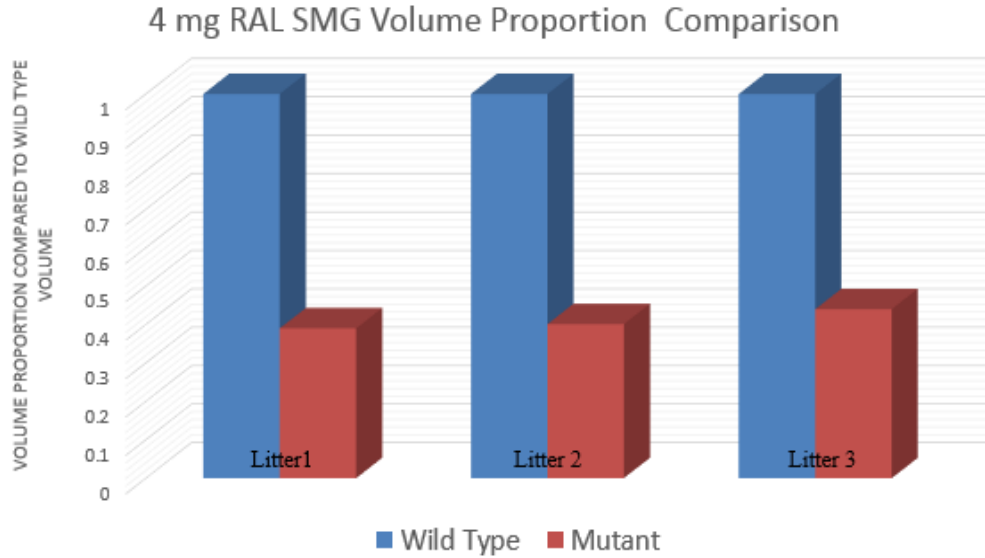


Figure 13. E13.5 SMGs whole mount statistical analysis. This figure shows a graphical representation of the E13.5 SMG volumes. Wild type SMG volume for each litter was normalized as the standard (blue). We can see that the mutants SMG volume (red) at E13.5 is about 45% that of the wild type's volume. N=3 separate litters for this volume analysis. The Wilcoxon Signed Rank Test was completed on these volumes, and verified a statistically significant difference between the mutant SMGs volume and the wild type SMG volume ($P < \alpha$, $0.091 < 0.10$).

Shown above in Fig.13, is the graphical representation of the whole mount volume analysis. Shown individually for each litter, the graph depicts the volume of the mutant SMG is about 40% compared to its wild type SMG volume. This method was used to account for variation in growth and development for each litter. By comparing a mutant to its corresponding wild type, we can know that the mutant and wild type were at identical stages of development.

In order to see if the SMGs grow in direct response to the dose of RA present, we repeated the volume analysis on embryos that were supplemented with a higher dose of RAL (fig.14). The same whole mount analysis was completed by looking at three separate litters, and comparing the mutant and wild type glands at E13.5 (fig.15).

As shown in Fig.15 the SMG of mutant embryos that received the higher dose of RAL are near the size of the wild type littermates. Note that this RAL dosage is not a full rescue, as many mutant embryos displayed many phenotypes of RA deficiency such as small forelimbs and orofacial clefts.

Vitamin A Metabolism

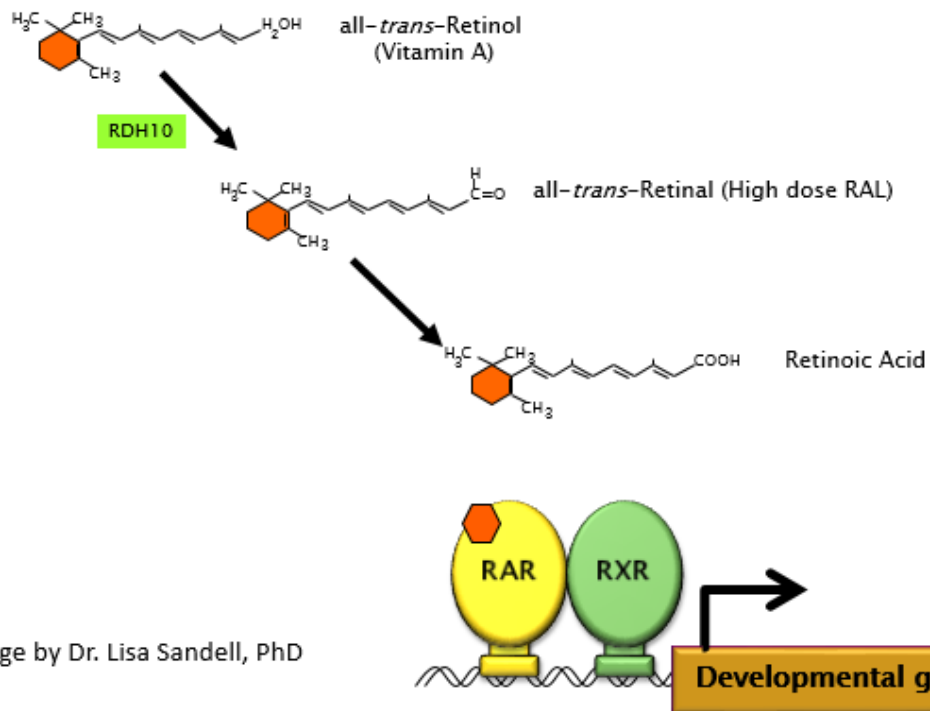


Image by Dr. Lisa Sandell, PhD

Figure 14. Vitamin A metabolism allows for adjustment and higher dosage of RAL. In order to see if the SMGs were impacted by the dose of RA, we increased the maternal supplementation of RAL to a higher dose (15 mg /g food/day). The amount of RAL given through the mother's diet was over tripled compared to the previous analysis at the low dose of RAL (4 mg/g food/day). Since we used RDH10^{tr_{ex}/tr_{ex}} RA deficient system, we can adjust the amount of RAL, and verify if this has an impact on the developing SMG.

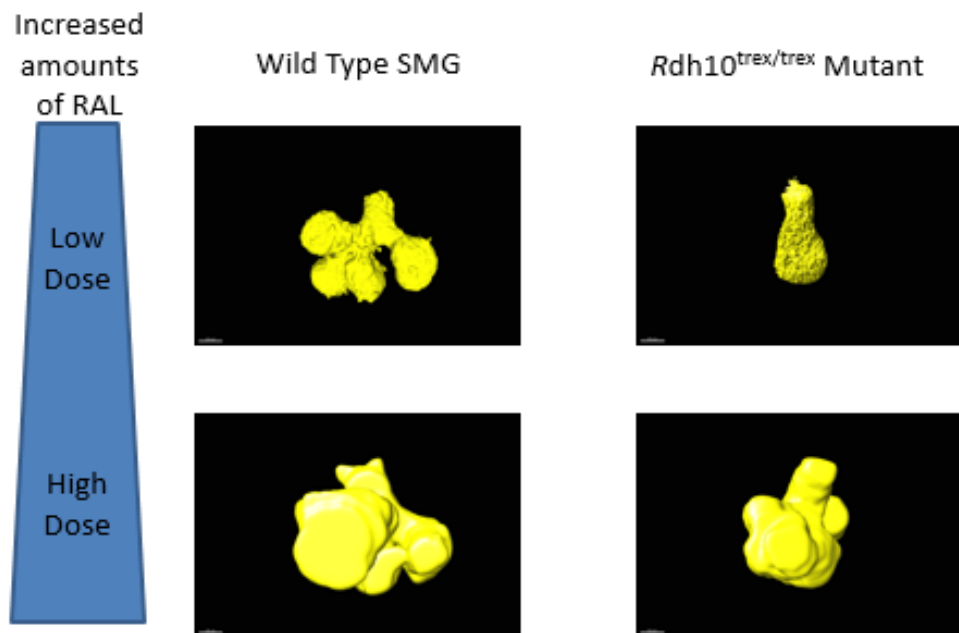


Figure 15. Increased amounts of RAL stimulated mutant SMG growth. This figure demonstrates that by increasing the amount of maternal supplementation of RAL the mutant SMGs grew better and appear to be closer to the wild type SMG size. These images are the 3D representation of the glands as formed by the Imaris software. N=3 separate litters for this analysis. The growth defect between the mutant and wild type SMG, was statistically significant as shown by the Wilcoxon Signed Rank test ($p < \alpha$, $0.091 < 0.10$).

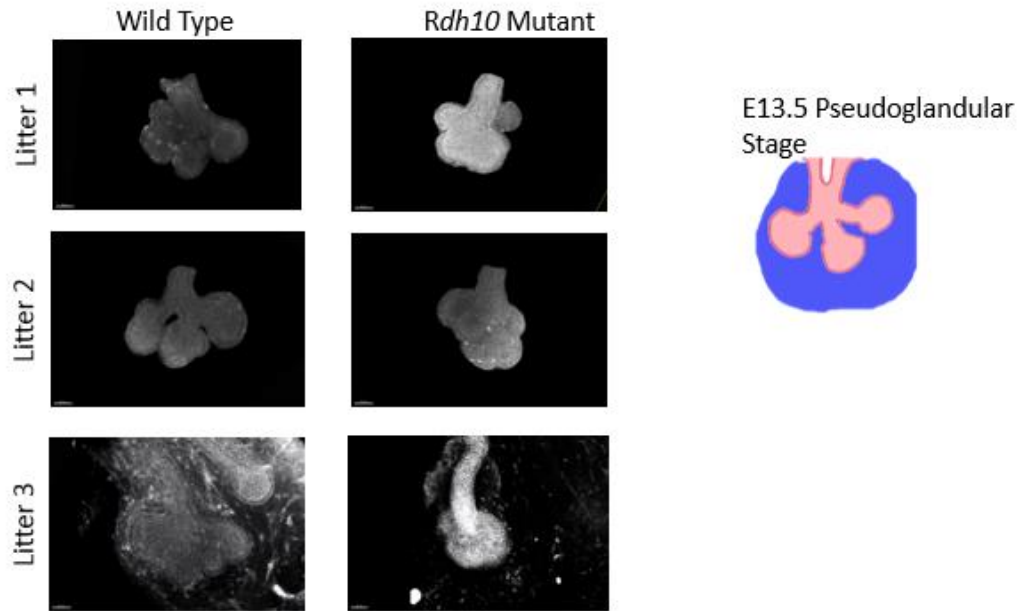
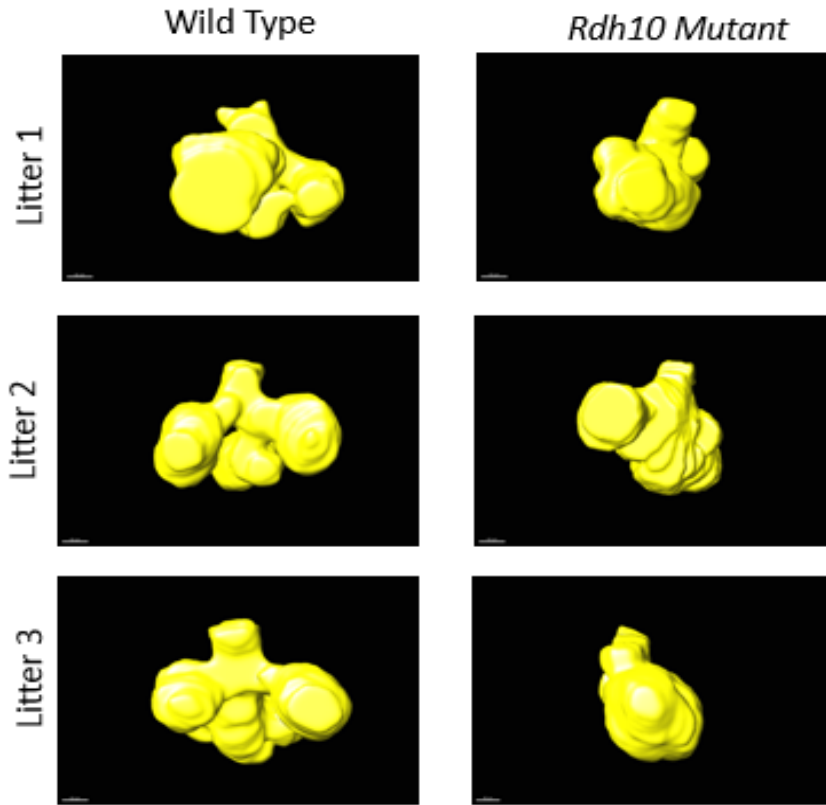


Figure 16. E13.5 SMGs whole mount images (high dose RAL). Shown above we see that the high dose of RAL allowed the mutant SMGs to grow better, closer to normal, than the low dose. This figure is a 2D representation based on the confocal Z stacks. Three different litters were studied (n=3). One wild type gland and one mutant gland were studied from each litter. The wild type is shown on the left and the corresponding mutant is on the right. Relative to the mutant SMG from the low dose RAL experiment, the mutant SMGs with the higher dose of RAL grew better and are closer to the size of their corresponding wild type.

Following the same procedure as for the low dose RAL treated glands, whole E13.5 SMGS were harvested. The glands were stained for E-cadherin and imaged on the confocal. The 3 litters and corresponding wild type and mutant glands are shown in fig. 16 (above). The mutant glands (on the right) are near the same size compared to their corresponding wild type glands (on the left). Volume of the glands was calculated by compiling the z stack from the confocal images, and the 3D representations are shown in Fig.17. Fig.17 also shows a table of the volumes of the SMGs as calculated by the Imaris Software. Fig.18 is the graphical representation of the E13.5 SMGs volumes. Normalizing the wild type SMGs volume and comparing their mutant's volume allows us to minimize the variation accounted for the difference in maturity and development among the litters. The data shows that the volume of the mutant SMG is about 75% compared to the wild type SMG volume. The Wilcoxon Signed Rank test was completed on the MiniTab software, and found that the p value (0.093) was less than the α value (0.10). Based on these test results, the difference between the mutant SMG volume and the wild type SMG volume is statistically significant.



15 mg RAL	litter 1	litter 2	litter 3
Wild Type Volume (μm^3)	2.32E+06	2.74E+06	2.05E+06
Mutant Volume (μm^3)	1.50E+06	1.92E+06	1.77E+06

Figure 17. E13.5 SMGs whole mount 3D images (high dose RAL). The above figure shows the 3D representation of the E13.5 SMGs. The 3D surface images are based on the compilation of the confocal z stacks, as formed by the Imaris Software. This analysis was completed on 3 separate litters of animals (n=3) and one wild type and one mutant from each litter was analyzed. Shown below the SMG images, are the actual volumes of each gland, as calculated by the software (units are μm^3).

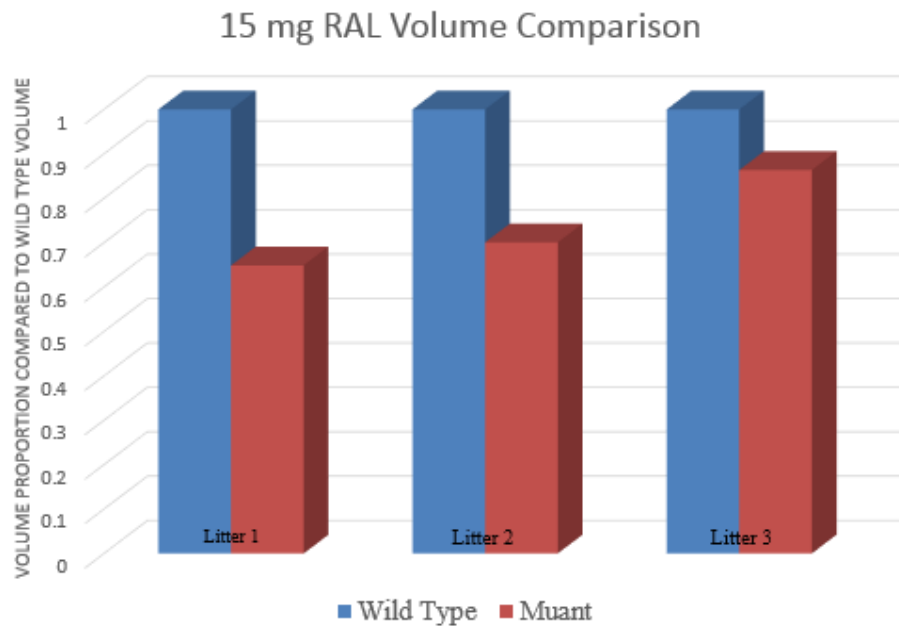


Figure 18. E13.5 SMGs whole mount statistical analysis (high dose RAL). This is the histogram of the volume of the E13.5 SMGs, as calculated by the Imaris program. The wild type volume for each litter was normalized and represents 1 (shown in blue). 3 different litters were studied for this analysis (n=3) and one wild type and one mutant SMG were used from each litter. Based on the graph, we see that the volume of high dose RAL mutant SMGs volume (red), is between 70%-80% the size of wild type littermates. The Wilcoxon Signed Rank test was completed, and verified a statistically significant difference between the mutant SMG volume and the wild type SMG volume. This test was completed with the program MiniTab, and found that the $p(0.093) < \alpha(0.10)$.

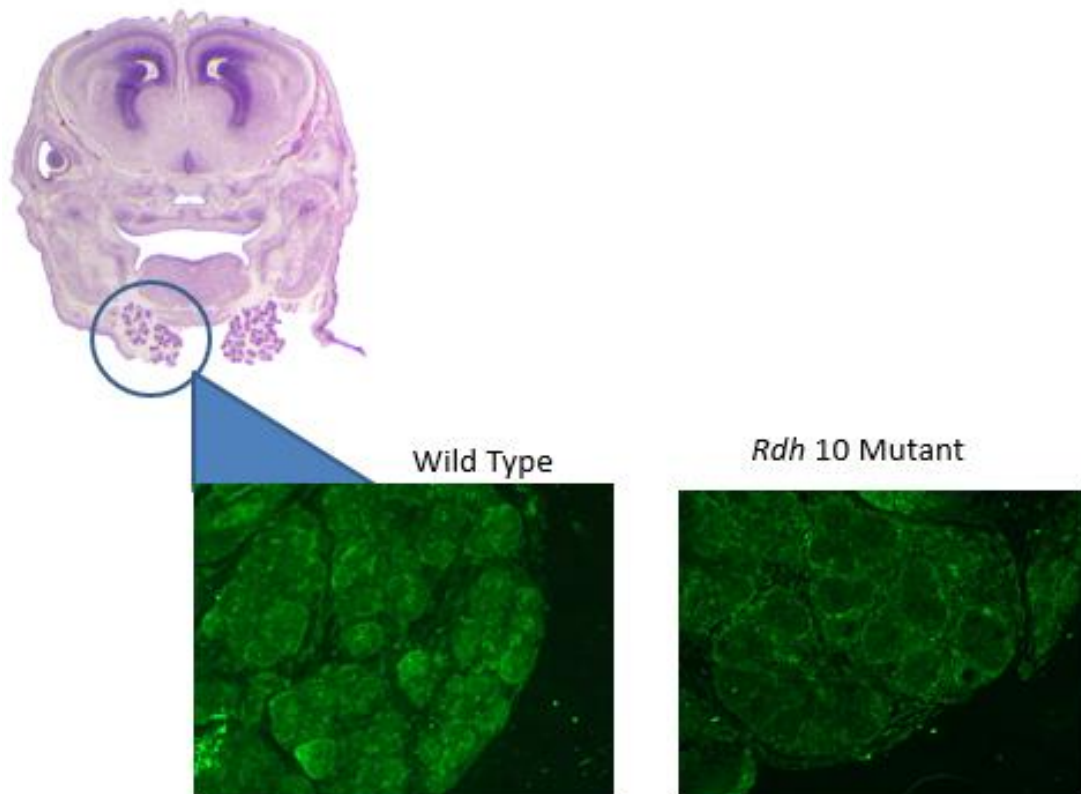


Figure 19. Immunofluorescence staining for PSP (Parotid Secreting Protein) on E15.5 SMGs. The above figure shows the immunofluorescence staining of E15.5 paraffin sections (treated with low dose RAL), stained for PSP on 10X magnification. This analysis was to see if the RA deficiency impacted the differentiation of the acinar cells in the mutant SMG compared to the wild type. By using the PSP antibody, we can assess the presence of differentiated cells and compare them to the mutant and wild type SMG. We see less differentiated cells in the mutant SMG compared to the wild type SMG.

Cell differentiation is an essential part of the development process. In order to assess if differentiation was impacted by the RA deficiency, we used an antibody to highlight differentiated acinar cells, PSP- Parotid Secreting Protein. PSP expression in the parotid gland is a sign of a terminally differentiated acini. The PSP protein has also been found in the perinatal SMGs, although expression levels diminish as the animal approaches adulthood [35, 36]. In figure 19 we see the PSP expression in the wild type on the left; on the right is shown the PSP expression in the *Rdh10^{trax/trax}* mutant SMG. These data indicate that the mutant SMG is less differentiated compared to the wild type SMG (fig.20).

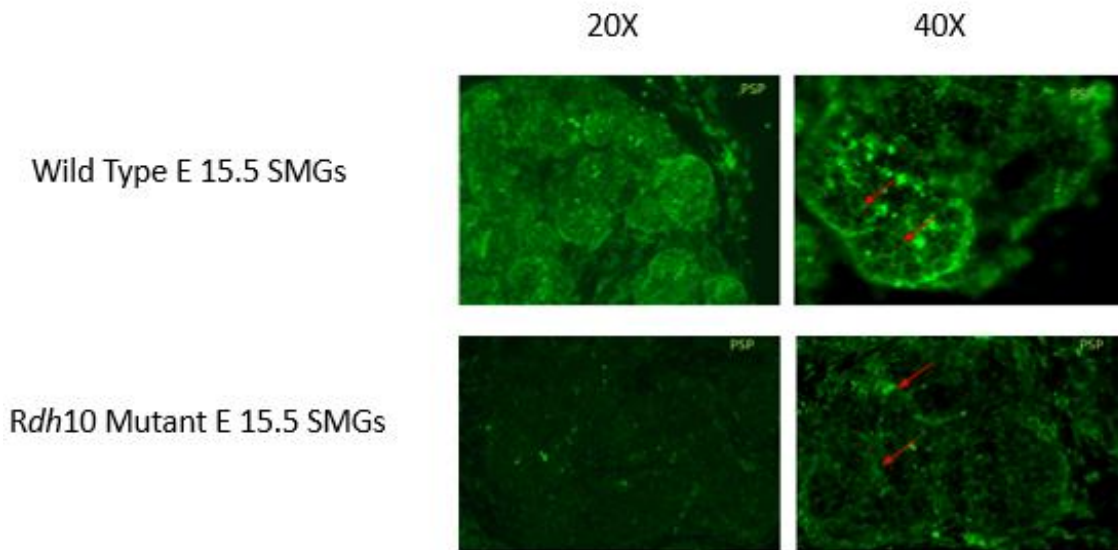


Figure 20. Immunofluorescence staining of PSP on E15.5 SMGs. This figure shows a 20X magnification of the E15.5 paraffin section SMGs on the left. On the right is the 40X magnification, and the red arrows demonstrate the expressing PSP cells. PSP staining was stronger in the wild type glands relative to the mutant glands. These data indicate that the mutant SMG is less differentiated than glands from wild type littermates. One wild type embryo and one mutant embryo were analyzed for this data.

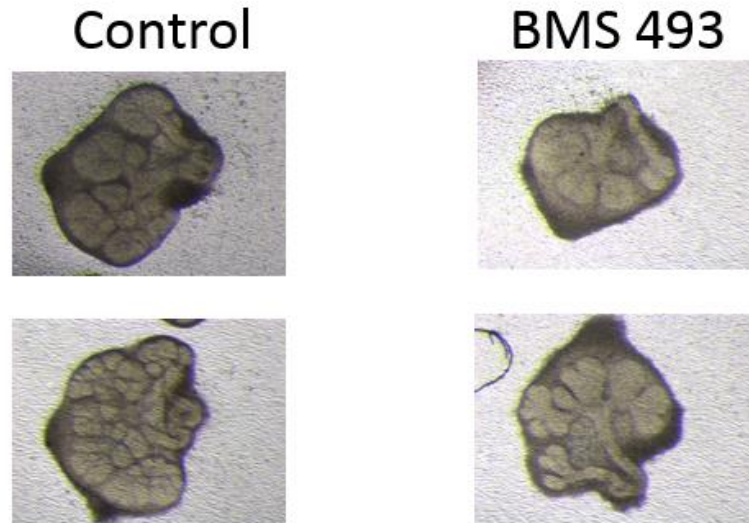


Figure 21. Cultured SMGs *in vitro* treated with RAR inhibitor (48 hrs.). The figure shows wild type glands cultured beginning at E13.5 for 48 hours. The control glands grew well and have more epithelium and branching compared to the BMS 493 treated glands. The BMS 493 treated glands were from the same corresponding animal on the left, and we see less branching and overall growth compared to the control SMGs. These are just two of the representative pairs of data, as this analysis was completed on 3 separate litters. N=21 glands for each group, control and treated SMGs.

In order to determine whether the effect of RA on the developing SMGs is direct, glands were cultured with and without synthetic RAR inhibitor. SMGs were harvested at E13.5 and were cultured for up to 3 days (72 hours). Half of the glands were treated with a synthetic pan-Retinoic Acid Receptor inhibitor – BMS493 diluted in DMSO, while contralateral glands were grown in control medium. The control medium received equivalent amounts of DMSO to account for the fact that the BMS 493 was suspended in DMSO. Shown above is a representative example of the progress of the SMGs after 48 hours grown in culture (fig.21). We see the controls on the left, and their corresponding treated glands on the right. BMS 493 is a synthetic pan-RAR inhibitor used to block the RAR in the developing glands. After 48 hours in culture, BMS 493 treated glands have less epithelial growth and branching compared to the control glands.

In order to quantify the effect of the RAR inhibitor at 48 hours in culture, the end buds were counted for both the control glands and the treated glands (table iii.) [37]. Depicted with red arrows, fig.22 demonstrates what was considered an end bud, and how these were counted on all the cultured glands. These data are the result of three individual experiments from three separate litters, and n=21 glands. Shown below, (fig.23) is the graphical representation of the end bud statistical analysis. The graph shows the average number of end buds for both the control and the treated SMGs, as well as error bars displaying the standard deviation from the collected data. Also shown, is a graph comparing the average end buds on the control and the treated cultured SMGs as a proportion (fig.24). We see from this data (table iii), that RA does have a direct effect on the developing SMGs. Specifically, the epithelium growth and branching is impacted when RA is blocked *in vitro*.

Control

BMS 493

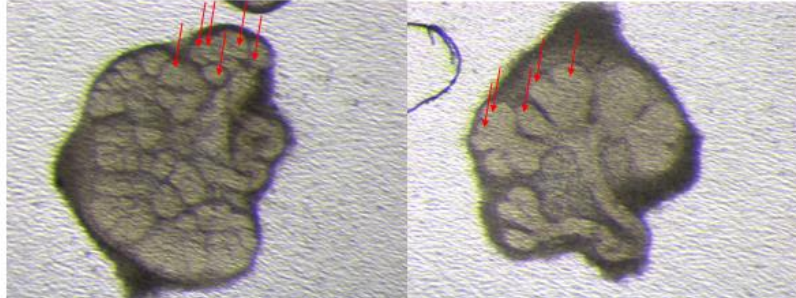


Figure 22. Counting end buds on cultured SMGs (48 hrs.). The above shows how the end buds were counted on the cultured SMGs for statistical purposes. Each individual section of epithelium was counted for both the control and BMS glands (depicted with a few red arrows). For this statistical analysis, n=21 control glands and n=21 treated glands from 3 separate projects. The t-test verifies statistical strength to this analysis as the p value (0.000066) is less than the α value (0.05).

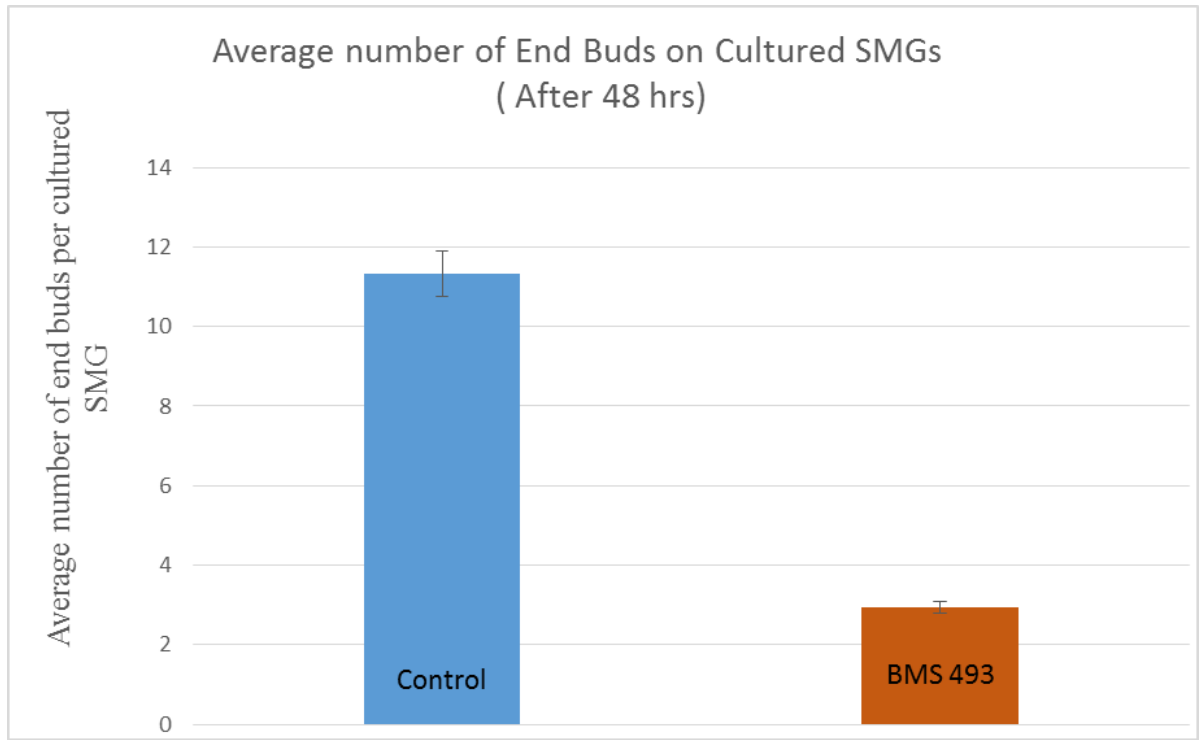


Figure 23. Statistical analysis of cultured SMGs (48 hrs.). The figure above shows the average number of end buds after 48 hours in culture for E13.5 SMGs. The control SMGs had an average of 11 end buds and the BMS 493 treated glands had an average of nearly four end buds per SMG ($n=21$ glands). The error bars demonstrate the standard deviation. A t-test was completed on this data, and the p value (0.000066) was less than the α value (0.05). Therefore, the t-test verifies that this data is statistically significant.

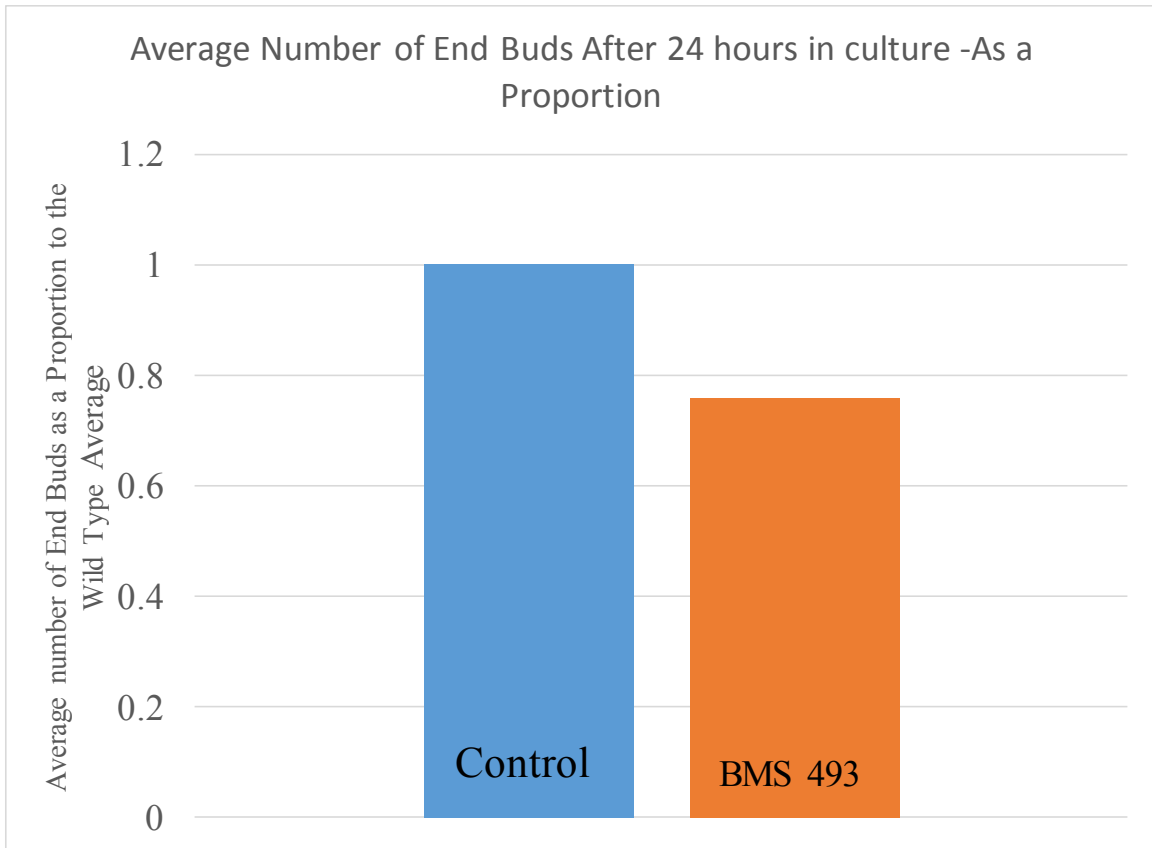
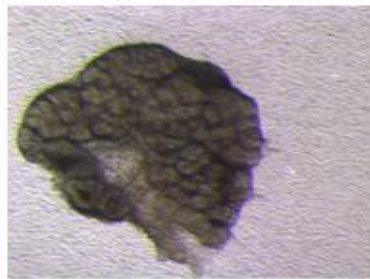
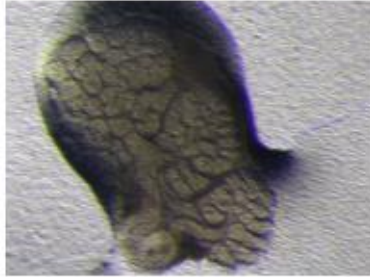


Figure 24. Statistical analysis of cultured glands (48 hours). This graph shows the average number of end buds for the control and the BMS 493 treated SMGs, with the end buds shown as a proportion. The average number of control end buds was normalized to 1, and we can see that the BMS 493 treated SMGs have about 30% the number of end buds of corresponding control glands. For this analysis, n=21 control SMGs and n=21 treated SMGs. A t-test was completed on this data and verified that the findings are statistically significant ($P < \alpha : 0.000066 < 0.05$).

Control



BMS

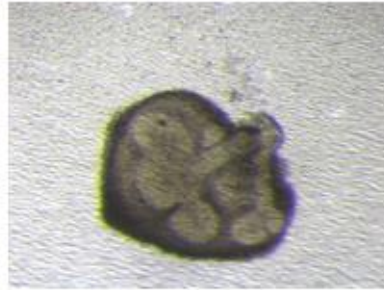


Figure 25. Cultured SMGs treated with RAR inhibitor (72 hrs.). This image shows that the variation between the control and BMS 493 treated glands is more obvious if the glands are cultured for 72 hours. At this stage, accurate counting end buds was not feasible, as the control SMG had healthy, robust branching. These are representative images of the collected data, and this experiment was completed 3 different times.

Shown above (fig.25) are some representative images from cultured glands after 3 days (72 hours) in culture. We see the growth defect of the RAR inhibited cultured SMGs is even more obvious as the glands continue to grow. Although statistical analysis was not completed on glands grown in culture for 72 hours, the experiment was completed on three separate litters, and the results were consistent.

After 48 hours in culture	BMS 493
Control	Treated
27	2
7	3
29	1
8	3
12	4
6	4
4	3
4	1
4	2
5	2
9	2
4	2
5	2
7	3
7	1
7	4
10	9
19	3
21	6
28	2
15	3
Average 11.33333	Average 2.952381

Table iii: Above is the end bud data for the cultured SMGs at 48 hours. This table shows the number of counted end buds per gland (n=21 control SMGs, n=21 treated SMGs). This data was collected from three different litters of animals. The average number of end buds per gland is shown at the bottom of the chart. This data is statistically significant as verified by a t-test, with the p value (0.000066) < α value (0.05). These data show that when RAR is inhibited in a cultured SMG, there is a statistically significant difference in the SMGs growth and differentiation (branching morphogenesis).

t-Test: Two-Sample Assuming Equal Variances

	<i>Variable</i> <i>1</i>	<i>Variable</i> <i>2</i>
Mean	11.33333	2.952381
Variance	70.93333	3.347619
Observations	21	21
Pooled Variance	37.14048	
Hypothesized Mean Difference	0	
Df	40	
t Stat	4.456196	
P(T<=t) one-tail	3.29E-05	
t Critical one-tail	1.683851	
P(T<=t) two-tail	6.57E-05	
t Critical two-tail	2.021075	

Table iv. T-test for cultured SMGs (48 hrs). This table shows the t-test results 48 hour cultured SMGs. n=21 control glands studied, and n=21 treated glands studied. This test verifies a statistically significant difference between the control glands average number of epithelial end buds and the treated glands average number of epithelial end buds. The p value (0.000066) is less than the α value (0.05), which says to reject the notion that there is no true difference between the two sets of data. Therefore, we can be assured that there is a statistically significant difference between the numbers of epithelial end buds per gland when comparing the control glands to the BMS treated glands at 48 hours in culture.

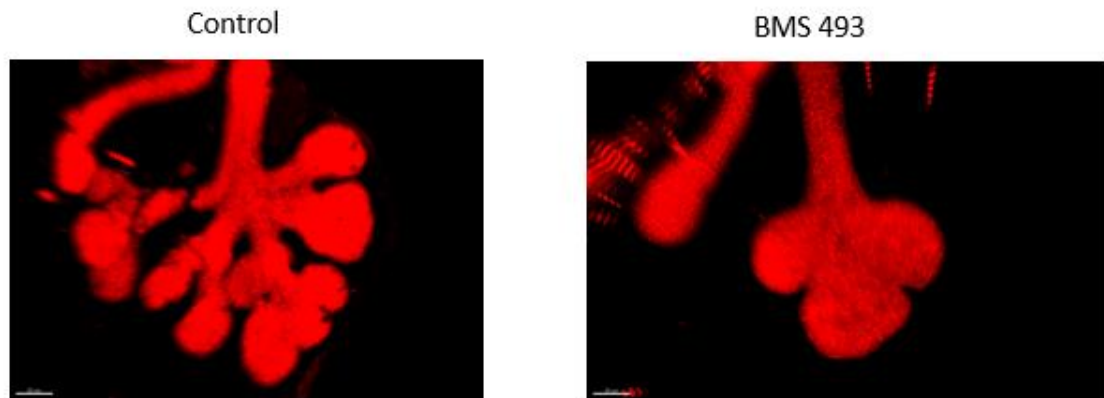


Figure 26. Immunofluorescence staining of cultured SMGs. The image above shows immunofluorescence of the SMG epithelium after 48 hours in culture. We see the control glands branched well and the epithelium grew, however the BMS 493 treated gland has minimal branching, a result of differentiation, and less epithelial growth.

Shown in fig. 27 is the epithelium immunofluorescence staining of a representative example of control and BMS 493-treated cultured SMGs. This method allows us to see the epithelium clearly, as we assess the variation between the control and the treated cultured glands. The control gland on the left, has numerous branches and more epithelium, whereas the gland on the right, looks near the size as an E13.5 SMG. The right gland is the gland treated with the RAR inhibitor, and we can see the growth defect in both amount of epithelium as well as in number of branching end buds. These images were taken on the confocal and are a 2D image from the z stack.

Shown below (fig.27) is the same pair of 48 hour cultured SMG stained with a marker of proliferating cells. The green fluorescence indicates phosphohistone 3 (PH3) expressing cells, which is a marker of cells actively in mitosis. This analysis was to see if the growth defect of the BMS-treated glands was a result of a decreased number of proliferating cells. Shown below are the confocal images for this analysis, including the 2D image from the Z stack representing the control (left) and treated gland (right).

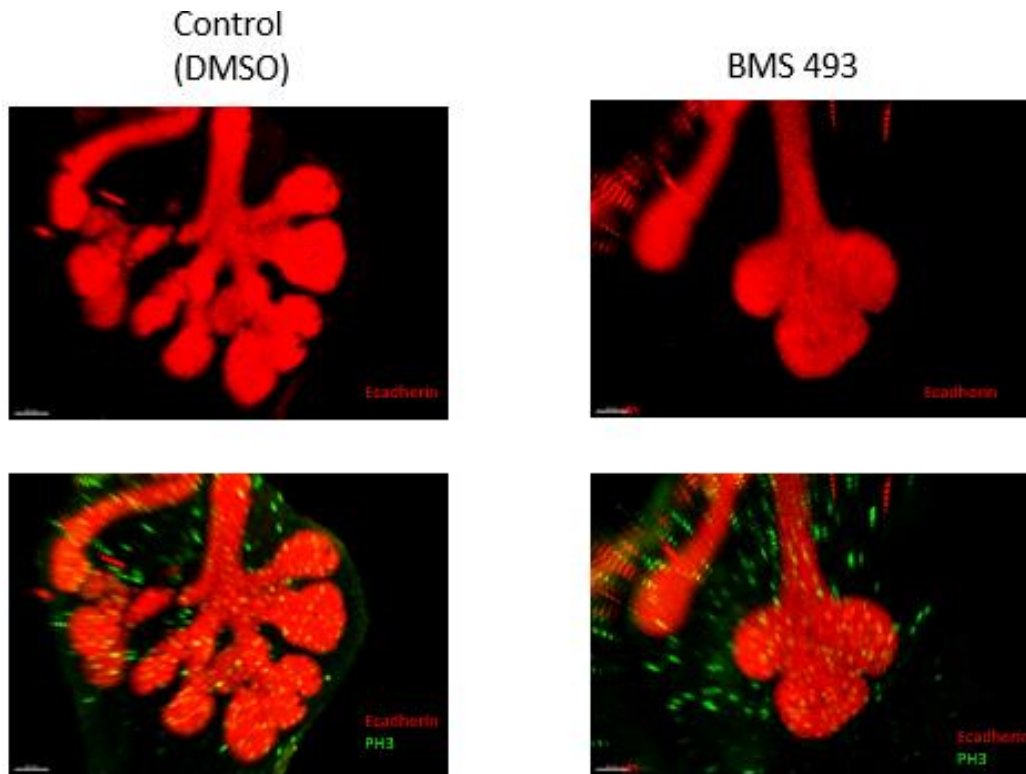


Figure 27. Immunofluorescence of cultured SMGs – both E-cadherin and PH3. This figure shows the immunofluorescence of the cultured E13.5 SMGs (48 hours *in vitro*). We see the epithelium depicted in red, and the PH3 expressing cells in green. These images were taken on the confocal laser microscope. It is clear to see that the SMG treated with BMS 493(right), has less epithelial growth as well as branching compared to the control gland (shown on the left).

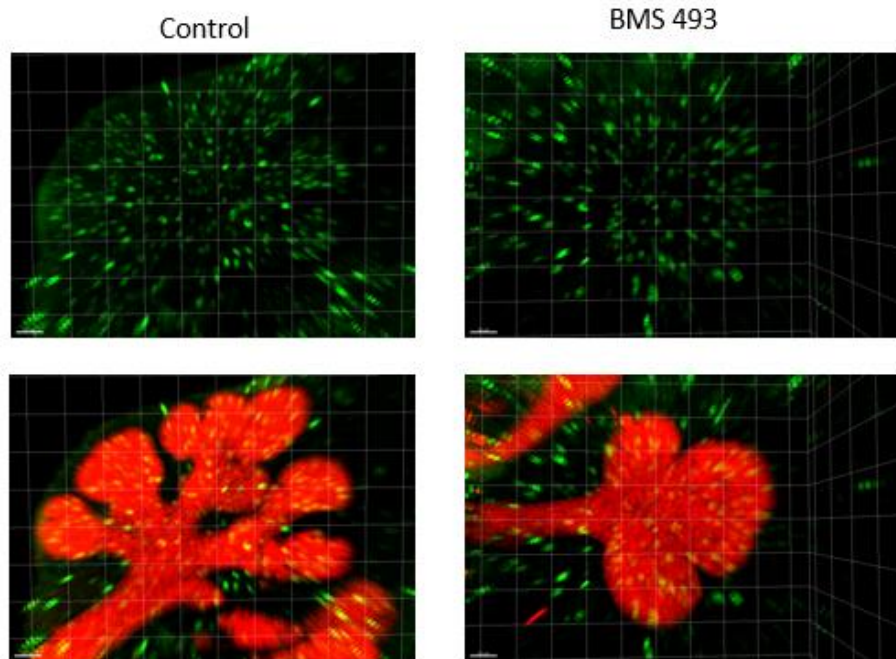
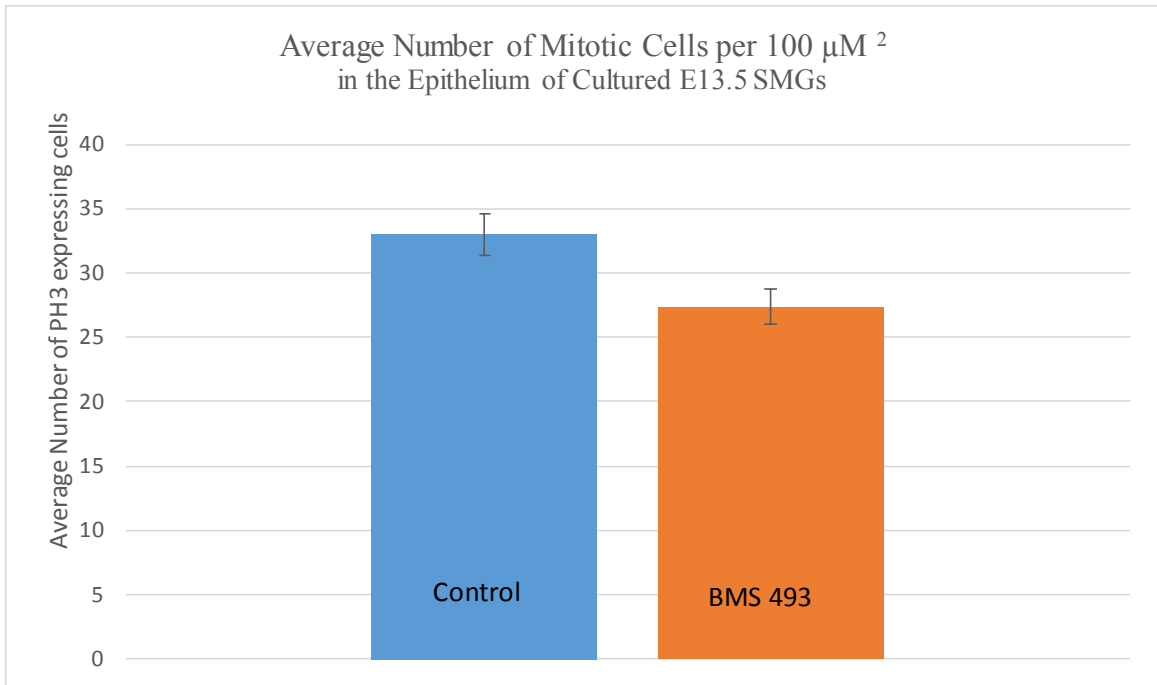


Figure 28. Quantifying cell proliferation in cultured control and BMS treated glands.

Using the Imaris program, we were able to form a grid on our confocal Z stack of the E13.5 cultured glands. This allowed the number of PH3 positive cells to be counted per 100 microns squared. Three different areas were studied for both the control gland and the treated gland (n=3). The number of PH3 expressing cells were counted for each area, and on average, there is less proliferating cells (PH3 expression) in the BMS 493 treated gland compared to the control gland.

In order to quantify the proliferating cells (PH3 expressing cells) on the 48 hour cultured and immunofluorescence stained cells, we formed a 3D image (fig.28) using the Imaris software we were able to overlay a grid on top of the gland images. Using this as a measurement tool, we could count the number of PH3 expressing cells per 100 micrometers squared, and compare the averages for both the control and the treated cultured SMG. Shown below is a graphical representation of the PH3 analysis of the immunofluorescence of the cultured SMGs (fig.29). We see that the average number of proliferating cells, based on three random fields of view, is lower in the BMS-treated gland compared to the control. This suggests that the growth defect in the BMS 493 treated cultured glands is because of less proliferating cells compared to the control gland. Further testing is necessary to give statistical strength to this finding, as this analysis was only completed on one pair of glands from the same embryo.



PH3 Analysis of the E13.5 Cultured SMGs

100 microns squared areas (100 μm^2)

Grid 1	30	29
Grid 2	41	29
Grid 3	28	24
Average	33	27

Figure 29. Statistical analysis of cultured control and treated SMGs. Above shows the average number of mitotic cells in the cultured glands per 100 microns squared. The error bars on the graph show the standard deviation, and 3 samples were used for this analysis (n=3). The chart shows the actual number of PH3 positive cells for the 3 grid regions that were randomly selected. Based on this preliminary data, the average number of mitotic cells (per 100 microns squared) is less in the BMS 493 treated gland compared to the control. Note that this analysis was completed on 1 pair of glands.

CHAPTER 4: DISCUSSION AND CONCLUSION

Saliva is necessary for the health of the oral tissues, prevention of tooth decay, and aiding in the processes of speech and digestion. Produced by the salivary glands, saliva is necessary for the basic function of the organism. In the case of hyposalivation, patients suffer discomfort, pain and a diminished quality of life as there is no effective treatment to reverse defective salivary glands. Xerostomia is the severe dry mouth condition that occurs as a result of the defective salivary glands, stemming from surgical damage, autoimmune disease or radiation therapy. Scientists are working toward bioengineering salivary glands from stem or progenitor cells in order to correct defective salivary glands. In order to direct stem cell growth towards differentiated and functional salivary gland tissues, first it must be fully understood how salivary glands form and develop in the embryo.

Vitamin A deficiency in embryonic salivary gland development has not been previously studied. By using the innovation of maternal RAL supplementation, we can use a RA deficient animal model and study the developing embryo's salivary glands under such conditions. Our data shows a reproducible growth defect in the SMGs of RA deficient embryos (fig. 5 and 8). This growth defect was present at the early stages of gland development such as the initial bud stage (E12.5) and is seen throughout the gland development (E13.5 and E 15.5). A small initial bud was seen in mutant embryos. This

suggests that RA is not absolutely essential for the invagination of the epithelium into the surrounding mesenchyme. Rather, RA is needed for growth and proliferation of the epithelium. In our mutant animals, RAL was administered at different doses, resulting in surviving embryos with smaller glands compared to its wild type counterpart.

Our analyses show the dosage of RA directly affects the SMG development. By increasing the maternal RAL supplementation from 4 mg to 15 mg, we observed that the increased RA stimulated SMG growth. This suggests a direct correlation between the amount of RA present and the epithelial growth of the SMG at E13.5.

We examined whether the growth defect of RA deficient SMGs might be associated with premature terminally differentiated cells. Based on preliminary data, the mutant SMG appears to have less terminally differentiated cells compared to the wild type SMG.

Our *in vitro* experiments with the SMGs show a direct effect on epithelial growth when the RA signaling was blocked with a chemical inhibitor. The SMGs that were treated with BMS 493, the synthetic pan-RAR inhibitor, displayed less epithelial growth and branching. This data clearly indicate that RA is necessary for branching and proliferation of the epithelium *in vitro*, demonstrating that RA directly affects the gland growth and branching of the gland in a culture dish.

In summary, our data show that RA has a direct affect on the development of the SMGs. RA is necessary for the branching and proliferation of the epithelium in the developing embryonic SMG. With minimal amounts of RA, we glands are smaller, with less branching and less cellular proliferation. This work can contribute towards understanding the complete picture of RA and its importance on the developing SMG.

These data can lend knowledge towards directing stem or progenitor cells to create a bioengineered salivary gland, offering a treatment for those who suffer with damaged salivary glands.

REFERENCES

1. Tucker, A.S., *Salivary gland development*. Semin Cell Dev Biol, 2007. **18**(2): p. 237-44.
2. Cheng, S.C., et al., *Assessment of post-radiotherapy salivary glands*. Br J Radiol, 2011. **84**(1001): p. 393-402.
3. Patel, V.N. and M.P. Hoffman, *Salivary gland development: a template for regeneration*. Semin Cell Dev Biol, 2014. **25-26**: p. 52-60.
4. Napenas, J.J. and T.S. Rouleau, *Oral complications of Sjogren's syndrome*. Oral Maxillofac Surg Clin North Am, 2014. **26**(1): p. 55-62.
5. Lubbers, H.T., A.L. Kruse, and D.A. Ettlin, *Postradiation xerostomia and oral pain*. J Am Dent Assoc, 2014. **145**(9): p. 964-5.
6. Kaluzny, J., et al., *Radiotherapy induced xerostomia: mechanisms, diagnostics, prevention and treatment--evidence based up to 2013*. Otolaryngol Pol, 2014. **68**(1): p. 1-14.
7. Cornec, D., C. Jamin, and J.O. Pers, *Sjogren's syndrome: where do we stand, and where shall we go?* J Autoimmun, 2014. **51**: p. 109-14.
8. Maslinska, M., et al., *Sjogren's syndrome: still not fully understood disease*. Rheumatol Int, 2014.
9. Patel, R. and A. Shahane, *The epidemiology of Sjogren's syndrome*. Clin Epidemiol, 2014. **6**: p. 247-55.
10. Grundmann, O., G.C. Mitchell, and K.H. Limesand, *Sensitivity of salivary glands to radiation: from animal models to therapies*. J Dent Res, 2009. **88**(10): p. 894-903.
11. Vissink, A., et al., *Current ideas to reduce or salvage radiation damage to salivary glands*. Oral Dis, 2014.
12. Lombaert, I.M., et al., *Rescue of salivary gland function after stem cell transplantation in irradiated glands*. PLoS One, 2008. **3**(4): p. e2063.
13. Ogawa, M., et al., *Functional salivary gland regeneration by transplantation of a bioengineered organ germ*. Nat Commun, 2013. **4**: p. 2498.
14. Feng, J., et al., *Isolation and characterization of human salivary gland cells for stem cell transplantation to reduce radiation-induced hyposalivation*. Radiother Oncol, 2009. **92**(3): p. 466-71.
15. Harunaga, J., J.C. Hsu, and K.M. Yamada, *Dynamics of salivary gland morphogenesis*. J Dent Res, 2011. **90**(9): p. 1070-7.
16. Wells, K.L., et al., *Dynamic relationship of the epithelium and mesenchyme during salivary gland initiation: the role of Fgf10*. Biol Open, 2013. **2**(10): p. 981-9.
17. Sakai, T., *Epithelial branching morphogenesis of salivary gland: exploration of new functional regulators*. J Med Invest, 2009. **56 Suppl**: p. 234-8.
18. Nedvetsky, P.I., et al., *Parasympathetic innervation regulates tubulogenesis in the developing salivary gland*. Dev Cell, 2014. **30**(4): p. 449-62.
19. Larsen, M., K.M. Yamada, and K. Musselmann, *Systems analysis of salivary gland development and disease*. Wiley Interdiscip Rev Syst Biol Med, 2010. **2**(6): p. 670-82.

20. Knox, S.M., et al., *Parasympathetic stimulation improves epithelial organ regeneration*. Nat Commun, 2013. **4**: p. 1494.
21. Ferreira, J.N. and M.P. Hoffman, *Interactions between developing nerves and salivary glands*. Organogenesis, 2013. **9**(3): p. 199-205.
22. Jaskoll, T., et al., *Sonic hedgehog signaling plays an essential role during embryonic salivary gland epithelial branching morphogenesis*. Dev Dyn, 2004. **229**(4): p. 722-32.
23. Jaskoll, T., et al., *FGF8 dose-dependent regulation of embryonic submandibular salivary gland morphogenesis*. Dev Biol, 2004. **268**(2): p. 457-69.
24. Maden, M., *Vitamin A and the developing embryo*. Postgrad Med J, 2001. **77**(910): p. 489-91.
25. Sandell, L.L., et al., *RDH10 is essential for synthesis of embryonic retinoic acid and is required for limb, craniofacial, and organ development*. Genes Dev, 2007. **21**(9): p. 1113-24.
26. Sandell, L.L., et al., *RDH10 oxidation of Vitamin A is a critical control step in synthesis of retinoic acid during mouse embryogenesis*. PLoS One, 2012. **7**(2): p. e30698.
27. Clagett-Dame, M. and H.F. DeLuca, *The role of vitamin A in mammalian reproduction and embryonic development*. Annu Rev Nutr, 2002. **22**: p. 347-81.
28. Mark, M., N.B. Ghyselinck, and P. Chambon, *Function of retinoic acid receptors during embryonic development*. Nucl Recept Signal, 2009. **7**: p. e002.
29. Clagett-Dame, M. and D. Knutson, *Vitamin A in reproduction and development*. Nutrients, 2011. **3**(4): p. 385-428.
30. See, A.W., et al., *A nutritional model of late embryonic vitamin A deficiency produces defects in organogenesis at a high penetrance and reveals new roles for the vitamin in skeletal development*. Dev Biol, 2008. **316**(2): p. 171-90.
31. Wolff, M.S., et al., *Development of the rat sublingual gland: a light and electron microscopic immunocytochemical study*. Anat Rec, 2002. **266**(1): p. 30-42.
32. Dardick, I., et al., *Submandibular gland adenocarcinoma of intercalated duct origin in Smgb-Tag mice*. Lab Invest, 2000. **80**(11): p. 1657-70.
33. Germain, P., et al., *Differential action on coregulator interaction defines inverse retinoid agonists and neutral antagonists*. Chem Biol, 2009. **16**(5): p. 479-89.
34. Lohnes, D., et al., *Developmental roles of the retinoic acid receptors*. J Steroid Biochem Mol Biol, 1995. **53**(1-6): p. 475-86.
35. Ball, W.D., L. Mirels, and A.R. Hand, *Psp and Smgb: a model for developmental and functional regulation in the rat major salivary glands*. Biochem Soc Trans, 2003. **31**(Pt 4): p. 777-80.
36. Ball, W.D., et al., *The B1-immunoreactive proteins of the perinatal submandibular gland: similarity to the major parotid gland protein, RPSP*. Crit Rev Oral Biol Med, 1993. **4**(3-4): p. 517-24.
37. Yang, T.L. and T.H. Young, *The enhancement of submandibular gland branch formation on chitosan membranes*. Biomaterials, 2008. **29**(16): p. 2501-8.

CURRICULUM VITAE

Deanna E. Buenger

Education:

- The University of Dayton

2009-2013

B.S. Pre dentistry

- The University of Louisville

2013-2015

M.S. Oral Biology Candidate